Figure 6. Specific sphingomyelin molecular species upregulated by HCV promote HCV replication on the detergent-resistant membrane fraction. (**A**) Comparison of the relative amounts of SM, as measured by MS analysis, in whole cells and the DRM fraction of mock-infected (HuH-7 K4 cells) (white, n = 6; whole cells, n = 3; DRM fraction) and HCV (JFH-1)-infected cells (JFH/K4 cells) (black, n = 6; whole cells, n = 3; DRM fraction). (**B**) Composition ratio of SM molecular species in whole cells and DRM fraction of HCV-infected cells. (**C**) Relative intensities of each SM molecular species in the DRM fraction of mock-infected cells (white, n = 2) and HCV-producing cells without (black, n = 2) or with NA808 treatment (gray, n = 2). (**D**) Results of the ELISA SM binding assay (n = 3 each). (**E**) Average activation kinetics of each SM molecular species on HCR6 (genotype 1b) RdRp (n = 3 each). (**F**) Scheme of HCV-RNA replicase assay using digitonin-permeabilized cells. (**G, H**) Effect of each SM molecular species on HCV-RNA in digitonin-permeabilized replicon cells treated without (G) or with 10 nM NA808 (H) (n = 3 each). In all cases, error bars indicate SDs. $*p<0.05$ and $**p<0.01$.
doi:10.1371/journal.ppat.1002860.g006

time course of acute HCV infection in cultured Huh-7.5 cells and observed that specific SM molecular species were decreased 72 h after HCV infection [27]. Given that their study focused on acute HCV infection, the reason for this discrepancy may be due to the severity of infection, suggesting that the influence of HCV infection on sphingolipid metabolism differs between acute and chronic infections. We also demonstrated that HCV infection correlates with increased abundance of specific SM and ceramide molecular species, with the profiles of individual lipids differing for infection by HCG9 (genotype 1a) and HCR24 (genotype 2a). The precise mechanism and meaning of these differences remain to be elucidated.

Our results indicated that SGMS1 expression had a correlation with HCV replication. This indicates that SM synthesized by SGMS1 contributes to HCV replication. A previous report revealed that in cultured cell lines, SGMS1 localizes in Golgi apparatus while SGMS2 localizes in the plasma membrane [28]. Thus, the results of this previous report suggest that SMs synthesized by SGMS1 can be easily incorporated into membranous replication complexes. As for SGMS2, we found that HCV infection significantly increased the expression of SGMS2, although the relationship between SGMS2 and HCV replication was hardly seen in this study. The relationship between SGMS2 and HCV propagation, thus, is an issue that should be elucidated in future studies.

We also demonstrated in this study that reduction of SM molecular species by NA808, a hepatotropic SPT inhibitor with little immunosuppressive activity, inhibits HCV replication in humanized chimeric mice regardless of viral genotype (Figure 4). Notably, treatment with NA808 (5 mg/kg) restored SM and ceramide levels in the liver to the levels observed in uninfected chimeric mice (Figure 5). Apparently, a slight reduction in SM had a significant influence on HCV, indicating that SM plays an important role in the HCV life cycle. SM is required for many viral processes in host-pathogen interactions [29–31]. For instance, viral envelopes of human immunodeficiency virus type 1 (HIV-1) and herpes simplex virus (HSV) are enriched with SM, which is necessary for efficient virus infectivity [32,33]. With regard to HCV, in addition to efficient virus infectivity [34], SM is present in the raft domain, which serves as a site of virus replication, together with other sphingolipids and cholesterol [6]. Moreover, SM is a component of VLDL whose assembly component and pathway is required for HCV morphogenesis and secretion [34,35]. The above-mentioned observations suggest that SM plays a multifaceted role in the HCV life cycle; therefore, SM is likely to be a good therapeutic target.

HCV is thought to replicate in a specialized compartment characterized as a DRM (designated as the membranous replication complex) [6]. SM, cholesterol, and phosphatidylinositol (PI) are thought to be the lipids that make up the membranous replication complex. With regard to PI, several siRNA screening have recently identified type III phosphatidylinositol 4-kinases (PI4K) as crucial host factors for HCV replication [36–39]. In HCV replicon containing cells, PI4P distribution is altered and enriched in the membranous replication complex by PI4KIIIα synthesis. Although the ability of PI to influence membrane bending and regulate intracellular processes (e.g. vesicle fusion, budding, and sorting) has been reported, the role of PI4P in the formation of the membranous replication complex remains to be elucidated. SM and cholesterol organize the solid membrane characterized as the DRM, where HCV replicates [6]. In fact, we and other groups demonstrated that reduction of SM and cholesterol suppressed HCV replication [7,9,12,40]. We performed the immunofluorescent analysis using lysenin. However, lysenin did not co-localize with NS4B protein. To date, it has been reported that lysenin-binding to SM is increased in the form of SM clusters, and that glycosphingolipids hinder lysein-binding to SM [41] Lipid rafts form of HCV replication complex do not have the characters of lysenin-binding to SM.

Further, the role of SM is not only to act as a constituent of the membranous replication complex, but also to bind and activate RdRp [7,8]. In this study, to gain further insight into the HCV membranous replication complex, we attempted to analyze which SM molecular species comprise the membranous replication complex, given that the diversity of molecular species is believed to be responsible for the physiochemical properties of the biomembrane [42] (Figure 6). We found that the composition ratio of SM molecular species observed in this study was quite different between the whole cell and DRM fractions. Further, to identify whether these SM molecular species contribute to HCV replication, we conducted rescue experiments using HCV replicon-containing cells (carrying intact RdRp and active membranous replication complexes) in which each SM molecular species was extrinsically added to replicon cells treated with NA808. However, in this experiment, addition of SM caused cell death. Therefore, we used digitonin-permeabilized semi-intact replicon cells, which enabled us to deliver the extrinsically added SM molecular species directly to the cytosol without catalytic effect and permitted monitoring of intact RdRp and replication complexes. We demonstrated that the specific endogenous SM molecular species (*d*18:1-16:0 and *d*18:1-24:0) enhance HCV-RNA replication, these species being consistent with the two SM molecular species which mainly constitute the DRM. Collectively, these results suggest that the HCV replication complex characterized as DRM is the specialized compartment that is composed of SM molecular species. These findings will provide new insights into the formation of the HCV replication complex and the involvement of host lipids in the HCV life cycle.

Materials and Methods

Ethics statement

This study was carried out in strict accordance with both the Guidelines for Animal Experimentation of the Japanese Association for Laboratory Animal Science and the recommendations in the Guide for the Care and Use of Laboratory Animals of the National Institutes of Health. All protocols were approved by the ethics committee of Tokyo Metropolitan Institute of Medical

Science. The patient with HCV infection who provided the serum samples gave written informed consent before blood collection.

Cells

The HCV subgenomic replicon cells FLR3-1 (genotype 1b, Con-1) was cultured at 37°C in Dulbecco's modified Eagle's medium GlutaMax-I (Invitrogen, Carlsbad, CA, USA) supplemented with 10% fetal bovine serum (FBS) and 0.5 mg/mL G418. HuH-7 K4 cells (cured of HCV by IFN treatment) and the JFH/K4 cells persistently infected with the HCV JFH-1 strain were maintained in DMEM containing 10% FCS and 0.1 mg/mL penicillin and streptomycin sulfate. MH-14 cells were grown in Dulbecco's modified Eagle's medium supplemented with 10% fetal bovine serum, 100 U/mL nonessential amino acids, 0.1 mg/mL penicillin and streptomycin sulfate, and 0.5 mg/mL G418.

siRNA assay

siCONTROL, siSGMS1, and siSGMS2 were purchased from Dharmacon RNA Technologies (Lafayette, CO, USA). The siCONTROL Non-Targeting siRNA #3 was used as the negative control siRNA. We used siRNAs against the HCV genome (siE-R7) [16]. The chemically synthesized siRNAs were transfected into cells using Lipofectamine RNAiMAX (Invitrogen) and Opti-MEM (Invitrogen) by reverse-transfection. Cells were characterized at 96 h after transfection.

Serine palmitoyltransferase activity

We assessed SPT activity in the liver as previously described, with minor modifications [43]. Briefly, frozen cells were homogenized in HEPES buffer (10 mM HEPES, 2 mM sucrose monolaurate, and 0.25 M sucrose, pH 7.4), and homogenates were centrifuged at 10,000×*g* for 20 min. From the resulting supernatant, samples containing 200 μg protein were assayed for SPT activity using [^{14}C]-serine and palmitoyl-CoA (Sigma-Aldrich, St. Louis, MO, USA) as substrates.

Proliferation assay

Human peripheral blood cells (AllCells, Emeryville, CA, USA) were plated onto 96-well plates and treated with phytohemagglutinin with or without immunosuppressant reagents. After 2 days of stimulation, [^{3}H]-thymidine-containing growth medium was added, and the cultures were incubated for another 18 h. T-cell proliferation was assessed by comparing the level of thymidine incorporation to that in the stimulated control.

Anti-hepatitis C virus assay in Huh-7 cells harboring subgenomic replicons

Replication was determined after 72 h with a Bright-Glo luciferase assay kit (Promega, Madison, WI, USA). The viability of replicon cells was determined using a cell counting kit (Dojindo, Kumamoto, Japan) according to the manufacturer's instructions.

Western blot analysis

Cells were resuspended in lysis buffer (10 mM Tris, pH 7.4 containing 1% SDS, 0.5% Nonidet P-40, 150 mM NaCl, 0.5 mM EDTA, and 1 mM dithiothreitol). Ten micrograms of the resulting protein sample were electrophoresed on a 10% sodium dodecyl sulfate-polyacrylamide gel and subsequently transferred to a polyvinylidene difluoride membrane (Immobilon-P; Millipore, Billerica, MA, USA). HCV nonstructural protein 3 (NS3) and nonstructural 5B polymerase (RdRp) were detected with rabbit anti-NS3 polyclonal antibody (R212) and mouse anti-RdRp monoclonal antibody (5B-14) prepared in our laboratory. β-Actin was detected with anti-β-actin monoclonal antibody (Sigma-Aldrich).

Immunofluorescent staining of hepatitis C virus replicon cells

After treatment with 25 nM NA808 for 96 h, FLR3-1 cells were probed with anti-NS3 polyclonal antibody (R212; the primary antibody). Next, an anti-rabbit IgG-Alexa 488 conjugate (Invitrogen) was applied as the secondary antibody.

Thin-layer chromatography analysis

Thin-layer chromatography (TLC) analysis was performed as described previously [9]. Briefly, cells were incubated with [^{14}C]-serine in Opti-MEM (Invitrogen). Cells extracts were obtained using the Bligh & Dyer method [44] and were spotted onto Silica Gel 60 TLC plates (Merck, Darmstadt, Germany) for separation. Radioactive spots were detected using a BAS 2000 system (Fuji Film, Kanagawa, Japan).

Membrane flotation assay

Cells were lysed in TNE buffer (25 mM Tris-HCl, 150 mM NaCl, 1 mM EDTA) and passed 20 times through a 25-gauge needle. Nuclei and unbroken cells were removed by centrifugation at 1,000×*g* for 5 min. After ensuring that the amount of total protein was equivalent across all samples, cell lysates were treated with 1% Triton on ice for 30 min and then subjected to a sucrose gradient (10%, 30%, and 40%). The sucrose gradient was centrifuged at 247,220×*g* in a Beckman SW41 Ti rotor (Beckman Coulter Inc., Brea, CA, USA) for 14 h at 4°C. Fractions (1 mL) were collected from the top of the gradient.

Infection of mice with hepatitis C virus genotypes 1a and 2a

Chimeric mice infected with HCV were prepared as previously described [45]. Briefly, approximately 40 days after the transplantation procedure, mice were intravenously injected with 5×10^5 copies/mouse of HCG9 (genotype 1a) or HCR24 (genotype 2a) that had been collected from patient serum.

Quantification of HCV RNA by real-time polymerase chain reaction

Total RNA was purified from 1 μL of chimeric mouse serum using SepaGene RV-R (Sanko Junyaku Co. Ltd., Tokyo, Japan) and from liver tissue using Isogene (Nippon Gene Co. Ltd., Tokyo, Japan). HCV RNA was quantified by quantitative real-time polymerase chain reaction (PCR) using previously reported techniques [9]. For serum, this technique has a lower limit of detection of 4000 copies/mL. Therefore, samples in which HCV RNA was undetectable were assigned this minimum value.

Quantification of HCV core protein by ELISA

Liver specimens were homogenized in TNE buffer. Aliquots of 5 μg of total protein were assayed for core protein levels with an Ortho HCV core protein ELISA kit (Eiken Chemical, Tokyo, Japan).

Indirect immunofluorescence analysis

The primary antibody for immunofluorescence analysis of liver sections was anti-HCV core protein monoclonal antibody (5E3) [46]. Monoclonal antibody labeling was followed by staining with anti-mouse IgG Alexa-488. The nuclei were stained using 4′,6-diamidino-2-phenylindole (DAPI).

Gene expression analysis

To measure mRNA levels, total RNA samples were extracted from the mouse livers and cDNA was synthesized using a High-Capacity cDNA Reverse Transcription Kit (Applied Biosystems, Foster City, CA, USA). The cDNA solution was assessed by quantitative PCR performed with TaqMan Gene Expression Assays (Applied Biosystems) and an ABI 7700 Sequence Detection System (Applied Biosystems).

Quantification of SM and ceramide in liver

We quantified liver SM and ceramide levels using a mass spectrometer (MS). Electrospray ionization (ESI)-MS analysis was performed using a 4000Q TRAP quadrupole-linear ion trap hybrid MS (AB SCIEX, Foster City, CA, USA) with an UltiMate 3000 nano/cap/micro-liquid chromatography system (Dionex Corporation, Sunnyvale, CA, USA) combined with an HTS PAL autosampler (CTC Analytics AG, Zwingen, Switzerland). The total lipid fractions expected to contain SM and ceramide, were subjected directly to flow injection and were selectively analyzed by neutral loss scanning of 60 Da (HCO_2+CH_3) from SM $[M+HCOO]^-$ in the negative ion mode, and multiple-reaction monitoring using a combination of ceramide $[Cer-H_2O+H]^+$ and the product (long-chain base) $[LCB-H_2O+H]^+$ in the positive ion mode [47,48]. The mobile phase composition was acetonitrile:methanol:water at 6:7:2 (0.1% ammonium formate, pH 6.8) and a flow rate of 10 μL/min. The typical injection volume was 3 μL of total lipids, normalized by protein content.

LC/ESI-MS analysis was performed using quadrupole/time of flight (Q-TOF) micro with an ACQUITY UPLC system (Waters Corporation, Milford, MA, USA) in the negative ion mode and an Agilent 6230 with an Agilent 1290 Infinity LC system (Agilent Technologies, Inc., Loveland, CO, USA) in the positive ion mode. Reversed-phase LC separation was achieved using an ACQUITY UPLC BEH column (150 mm×1.0 mm i.d., Waters Corporation) at 45°C. The mobile phase was acetonitrile:methanol:water at 19:19:2 (0.1% formic acid+0.028% ammonia) (A) and isopropanol (0.1% formic acid+0.028% ammonia) (B), and the composition was produced by mixing these solvents. The gradient consisted of holding A:B at 90:10 for 7.5 min, then linearly converting to A:B at 70:30 for 32.5 min, and then linearly converting to A:B at 40:60 for 50 min. The detailed procedure for LC/ESI-MS was described previously [49,50].

Separation of SM molecular species by HPLC

Bovine milk or brain SM (Avanti Polar Lipids. Inc., Alabaster, AL, USA) was dissolved in chloroform:methanol (2:1), then separated according to molecular species by reversed-phase HPLC. The *d*18:1-16:0, 22:0, and 24:0 molecular species of SM were isolated from bovine milk SM, while the *d*18:1-24:0 and 24:1 molecular species were isolated from brain SM. Bovine milk and brain SM were then separated on Senshu PAK ODS (C18) columns (Senshu Scientific Co., Ltd., Tokyo, Japan) using methanol as the eluting solvent at a flow rate of 1 mL/min. The fatty acid compositions of the purified fractions were analyzed by LC/ESI-MS. The amount of SM in each fraction was quantified using an SM assay kit (Cayman Chemical, Ann Arbor, MI, USA). We confirmed that the purity of each molecular species was approximately 90% without *d*18:1-24:1 (about 70%) (data not shown).

In vitro HCV transcription

In vitro HCV transcription was performed as previously described [8].

SM binding assay using ELISA

An SM binding assay was performed as previously described [8] using rabbit anti-HCV RdRp sera (1:5000) and an HRP-conjugated anti-rabbit IgG antibody (1:5000). Optical density at 450 nm (OD_{450}) was measured on a Spectra Max 190 spectrophotometer (Molecular Devices, Sunnyvale, CA, USA) using the TMB Liquid Substrate System (Sigma).

RNA replication assays in permeabilized replicon cells

The analysis using digitonin-permeabilized replicon cells was performed as previously described [20] with minor modifications. Briefly, MH-14 cells of about 80% confluency were pre-cultured for 2 h in complete Dulbecco's modified Eagle's medium containing 5 μg/mL actinomycin D (Nacalai Tesque, Kyoto, Japan), then washed with cold buffer B (20 mM HEPES-KOH (pH 7.7 at 27°C), 110 mM potassium acetate, 2 mM magnesium acetate, 1 mM EGTA, and 2 mM dithiothreitol). The cells were permeabilized by incubation in buffer B containing 50 μg/mL digitonin for 5 min at 27°C, and the reaction was stopped by washing twice with cold buffer B. The permeabilized cells were then incubated for 4 h at 27°C in the reaction mixture with or without each lipid. The reaction mixture consisted of 2 mM manganese(II) chloride, 1 mg/mL acetylated bovine serum albumin (Nacalai Tesque), 5 mM phosphocreatine (Sigma), 20 units/mL creatine phosphokinase (Sigma), 50 μg/mL actinomycin D, and 500 μM each of ATP, CTP, GTP, and UTP (Roche Diagnostics, Basel, Switzerland) in buffer B (pH 7.7). Total RNA was purified by the acid guanidinium-phenol-chloroform method. In this assay, considering that the estimated SM content in human hepatocytes is 3–4 nmol/mg protein, as demonstrated by MS analysis (**Figure S10**), the amount of SM we added in the replicase assay was 0.3–1 μM. (i.e. 0.03–0.3 nmol/0.3 mL/0.1 mg protein/12 well; the reaction volume in the replicase assay was 0.3 mL/12 wells and each well of the 12 well cell culture plates contained approximately 0.1 mg protein.)

Statistical analysis

Statistical analysis was performed using the Student's *t*-test equipped with Excel 2008 (Microsoft, Redmond, WA, USA). To measure the strength of the association, Pearson correlation coefficient was calculated using Excel 2008. A p-value<0.05 was considered statistically significant.

Supporting Information

Figure S1 Impacts of HBV infection on expression of sphingomyelin (SM) biosynthesis genes. mRNA expression of *SGMS1* and *SGMS2* genes (encoding SM synthases 1 and 2, respectively) in uninfected (white) and infected (black) chimeric mice (n = 5 per group).
(JPG)

Figure S2 Effect of HCV infection in cultured cells. Comparison of the relative amounts of SM, as measured by MS analysis, in mock-infected (HuH-7 K4 cells) (white) and HCV (JFH-1)-infected cells (JFH/K4 cells) (black) (n = 1 per group).
(JPG)

Figure S3 The expression of HCV core protein in HCV-infected chimeric mice. Histological analysis using immunohistochemical labeling of HCV core protein.
(JPG)

Figure S4 Effects of NA808 on HCV-infected chimeric mice. (**A**) Average body weight of mice during treatment. (**B**) Average human albumin concentrations in the sera of mice during

treatment. (**C**) Histological analysis using H&E staining and immunofluorescent labeling of human albumin (red). In all cases, error bars indicate SDs.
(JPG)

Figure S5 Concentrations of NA808 in chimeric mice receiving NA808 treatment. Concentration of NA808 in the liver (gray) and serum (black) of chimeric mice treated with 5 mg/kg or 10 mg/kg NA808. Stars indicate that NA808 level was not detected.
(JPG)

Figure S6 Sphingomyelin (SM) levels in the serum of chimeric mice receiving NA808 treatment. SM levels in the serum of chimeric mice (n = 3 per group) that were uninfected (HCV−), or infected (HCV+) but untreated or treated with 5 or 10 mg/kg NA808. Error bars indicate SDs.
(JPG)

Figure S7 Effects of NA808 on associations between the HCV nonstructural 5B polymerase (RdRp) and sphingomyelin (SM). (**A**) Comparison of SDS-PAGE and TLC results for replicon cells receiving no treatment (Control) or NA808 treatment (NA808). NA808 dosage was 2.5 nM (for TLC) or 25 nM (for SDS-PAGE). (**B**) Relative band intensities of RdRp and NS3 in detergent-resistant membrane (DRM) fractions from cells receiving no treatment (Control) or 25 nM NA808 treatment (NA808). (**C**) Relative band intensities of SM in DRM fractions from cells receiving no treatment (Control) or 2.5 nM NA808 treatment (NA808).
(JPG)

Figure S8 Composition ratio of SM molecular species in whole cells and DRM fraction of uninfected cells.
(JPG)

Figure S9 Effect of NS3 protease inhibitor on SM molecular species in the DRM fractions of subgenomic replicon cells. (A) Effect of NS3 protease inhibitor (VX950) on HCV replication (dark grey bars) and cell viability (light grey bars) in FLR3-1 replicon-containing cells. Error bars indicate SD. (B) Effect of NS3 protease inhibitor (VX950; 3 μM) on SM molecular species of DRM fractions of FLR 3-1 replicon-containing cells. Error bars indicate SDs.
(JPG)

Figure S10 The estimated SM content in human hepatocytes. Left bar (white) indicates the intensity of SM internal standard (SM d18:0-12:0; 1 nmol) by mass spectrometer. Right bar indicates the intensity of 1 mg protein of human hepatocyte (HuH-7 K4).
(JPG)

Table S1 Distribution of radioactivity in tissues after a single intravenous administration of [^{14}C] NA808 at 2 mg/kg to non-fasting male rats.
(PDF)

Table S2 Treatment administration for HCV-infected chimeric mice. Administration of reagents was started at day 0. The amount of NA808 was adjusted according to the body weight of the mice. Dose began at 5 mg/kg or 10 mg/kg and was reduced by half at each 10% reduction in body weight (half circle). At 20% reduction, administration was discontinued. Open circle indicates each manipulation was performed as required.
(PDF)

Text S1 Materials and methods for supporting information. Methods for "Infection of chimeric mice with hepatitis B virus", "Quantification of human albumin", "Histological staining and indirect immunofluorescence analysis", and "Quantification of sphingomyelin (SM) in serum" are described.
(DOCX)

Acknowledgments

We are very grateful to Dr. Makoto Hijikata of the Department of Viral Oncology, Institute for Virus Research, Kyoto University for his technical support. We thank Isao Maruyama and Hiroshi Yokomichi of PhoenixBio Co., Ltd. for maintenance of and technical assistance with the chimeric mice.

Author Contributions

Conceived and designed the experiments: M. Kohara. Wrote the paper: Y. Hirata. Y. Hirata performed the experiment of chimeric mice and HCV-infected cells. K. Ikeda, M. Ohta, T. Soga, and R. Taguchi performed lipid analysis by MS spectrometry. M. Sudoh, A. Katsume, and Y. Aoki evaluated the antiviral effects of NA808, K. Okano and K. Ozeki examined the tissue distribution of NA808. K. Kawasaki and T. Tsukuda synthesized derivatives from natural compounds. Y. Tokunaga, Y. Tobita, T. Umehara, and S. Sekiguchi performed some experiments on the chimeric mice. L. Weng and T. Toyoda conducted the experiments on the interaction between RdRp and SM. M. Kohara and Y. Hirata performed data analysis on the chimeric mice and cells. K. Ikeda, M. Ohta, T. Soga, and R. Taguchi performed data analysis on the result of MS spectrometry. A. Suzuki, K. Shimotohno, and M. Nishijima provided tools and expert information.

References

1. Wenk MR (2006) Lipidomics of host-pathogen interactions. FEBS Lett 580: 5541–5551.
2. Brown DA, Rose JK (1992) Sorting of GPI-anchored proteins to glycolipid-enriched membrane subdomains during transport to the apical cell surface. Cell 68: 533–544.
3. Simons K, Toomre D (2000) Lipid rafts and signal transduction. Nat Rev Mol Cell Biol 1: 31–39.
4. van der Meer-Janssen YP, van Galen J, Batenburg JJ, Helms JB (2010) Lipids in host-pathogen interactions: pathogens exploit the complexity of the host cell lipidome. Prog Lipid Res 49: 1–26.
5. Aizaki H, Lee KJ, Sung VM, Ishiko H, Lai MM (2004) Characterization of the hepatitis C virus RNA replication complex associated with lipid rafts. Virology 324: 450–461.
6. Shi ST, Lee KJ, Aizaki H, Hwang SB, Lai MM (2003) Hepatitis C virus RNA replication occurs on a detergent-resistant membrane that cofractionates with caveolin-2. J Virol 77: 4160–4168.
7. Sakamoto H, Okamoto K, Aoki M, Kato H, Katsume A, et al. (2005) Host sphingolipid biosynthesis as a target for hepatitis C virus therapy. Nat Chem Biol 1: 333–337.
8. Weng L, Hirata Y, Arai M, Kohara M, Wakita T, et al. (2010) Sphingomyelin activates hepatitis C virus RNA polymerase in a genotype-specific manner. J Virol 84: 11761–11770.
9. Umehara T, Sudoh M, Yasui F, Matsuda C, Hayashi Y, et al. (2006) Serine palmitoyltransferase inhibitor suppresses HCV replication in a mouse model. Biochem Biophys Res Commun 346: 67–73.
10. Kapadia SB, Chisari FV (2005) Hepatitis C virus RNA replication is regulated by host geranylgeranylation and fatty acids. Proc Natl Acad Sci U S A 102: 2561–2566.
11. Su AI, Pezacki JP, Wodicka L, Brideau AD, Supekova L, et al. (2002) Genomic analysis of the host response to hepatitis C virus infection. Proc Natl Acad Sci U S A 99: 15669–15674.
12. Takano T, Tsukiyama-Kohara K, Hayashi M, Hirata Y, Satoh M, et al. (2011) Augmentation of DHCR24 expression by hepatitis C virus infection facilitates viral replication in hepatocytes. J Hepatol 55: 512–521.
13. Tateno C, Yoshizane Y, Saito N, Kataoka M, Utoh R, et al. (2004) Near completely humanized liver in mice shows human-type metabolic responses to drugs. Am J Pathol 165: 901–912.
14. Mercer DF, Schiller DE, Elliott JF, Douglas DN, Hao C, et al. (2001) Hepatitis C virus replication in mice with chimeric human livers. Nat Med 7: 927–933.

15. Valsecchi M, Mauri L, Casellato R, Prioni S, Loberto N, et al. (2007) Ceramide and sphingomyelin species of fibroblasts and neurons in culture. J Lipid Res 48: 417–424.
16. Watanabe T, Sudoh M, Miyagishi M, Akashi H, Arai M, et al. (2006) Intracellular-diced dsRNA has enhanced efficacy for silencing HCV RNA and overcomes variation in the viral genotype. Gene Ther 13: 883–892.
17. Fujita T, Inoue K, Yamamoto S, Ikumoto T, Sasaki S, et al. (1994) Fungal metabolites. Part 11. A potent immunosuppressive activity found in Isaria sinclairii metabolite. J Antibiot (Tokyo) 47: 208–215.
18. Miyake Y, Kozutsumi Y, Nakamura S, Fujita T, Kawasaki T (1995) Serine palmitoyltransferase is the primary target of a sphingosine-like immunosuppressant, ISP-1/myriocin. Biochem Biophys Res Commun 211: 396–403.
19. Park TS, Panek RL, Mueller SB, Hanselman JC, Rosebury WS, et al. (2004) Inhibition of sphingomyelin synthesis reduces atherogenesis in apolipoprotein E-knockout mice. Circulation 110: 3465–3471.
20. Miyanari Y, Hijikata M, Yamaji M, Hosaka M, Takahashi H, et al. (2003) Hepatitis C virus non-structural proteins in the probable membranous compartment function in viral genome replication. J Biol Chem 278: 50301–50308.
21. Diamond DL, Jacobs JM, Paeper B, Proll SC, Gritsenko MA, et al. (2007) Proteomic profiling of human liver biopsies: hepatitis C virus-induced fibrosis and mitochondrial dysfunction. Hepatology 46: 649–657.
22. Tardif KD, Mori K, Siddiqui A (2002) Hepatitis C virus subgenomic replicons induce endoplasmic reticulum stress activating an intracellular signaling pathway. J Virol 76: 7453–7459.
23. Pettus BJ, Chalfant CE, Hannun YA (2002) Ceramide in apoptosis: an overview and current perspectives. Biochim Biophys Acta 1585: 114–125.
24. Tepper AD, Ruurs P, Wiedmer T, Sims PJ, Borst J, et al. (2000) Sphingomyelin hydrolysis to ceramide during the execution phase of apoptosis results from phospholipid scrambling and alters cell-surface morphology. J Cell Biol 150: 155–164.
25. Liu YY, Han TY, Giuliano AE, Hansen N, Cabot MC (2000) Uncoupling ceramide glycosylation by transfection of glucosylceramide synthase antisense reverses adriamycin resistance. J Biol Chem 275: 7138–7143.
26. Taguchi Y, Kondo T, Watanabe M, Miyaji M, Umehara H, et al. (2004) Interleukin-2-induced survival of natural killer (NK) cells involving phosphatidylinositol-3 kinase-dependent reduction of ceramide through acid sphingomyelinase, sphingomyelin synthase, and glucosylceramide synthase. Blood 104: 3285–3293.
27. Diamond DL, Syder AJ, Jacobs JM, Sorensen CM, Walters KA, et al. (2010) Temporal proteome and lipidome profiles reveal hepatitis C virus-associated reprogramming of hepatocellular metabolism and bioenergetics. PLoS Pathog 6: e1000719.
28. Huitema K, van den Dikkenberg J, Brouwers JF, Holthuis JC (2004) Identification of a family of animal sphingomyelin synthases. EMBO J 23: 33–44.
29. Merrill AH, Jr., Schmelz EM, Dillehay DL, Spiegel S, Shayman JA, et al. (1997) Sphingolipids–the enigmatic lipid class: biochemistry, physiology, and pathophysiology. Toxicol Appl Pharmacol 142: 208–225.
30. Huwiler A, Kolter T, Pfeilschifter J, Sandhoff K (2000) Physiology and pathophysiology of sphingolipid metabolism and signaling. Biochim Biophys Acta 1485: 63–99.
31. Hannun YA, Luberto C, Argraves KM (2001) Enzymes of sphingolipid metabolism: from modular to integrative signaling. Biochemistry 40: 4893–4903.
32. van Genderen IL, Brandimarti R, Torrisi MR, Campadelli G, van Meer G (1994) The phospholipid composition of extracellular herpes simplex virions differs from that of host cell nuclei. Virology 200: 831–836.
33. Brugger B, Glass B, Haberkant P, Leibrecht I, Wieland FT, et al. (2006) The HIV lipidome: a raft with an unusual composition. Proc Natl Acad Sci U S A 103: 2641–2646.
34. Aizaki H, Morikawa K, Fukasawa M, Hara H, Inoue Y, et al. (2008) Critical role of virion-associated cholesterol and sphingolipid in hepatitis C virus infection. J Virol 82: 5715–5724.
35. Syed GH, Amako Y, Siddiqui A (2010) Hepatitis C virus hijacks host lipid metabolism. Trends Endocrinol Metab 21: 33–40.
36. Berger KL, Cooper JD, Heaton NS, Yoon R, Oakland TE, et al. (2009) Roles for endocytic trafficking and phosphatidylinositol 4-kinase III alpha in hepatitis C virus replication. Proc Natl Acad Sci U S A 106: 7577–7582.
37. Borawski J, Troke P, Puyang X, Gibaja V, Zhao S, et al. (2009) Class III phosphatidylinositol 4-kinase alpha and beta are novel host factor regulators of hepatitis C virus replication. J Virol 83: 10058–10074.
38. Tai AW, Benita Y, Peng LF, Kim SS, Sakamoto N, et al. (2009) A functional genomic screen identifies cellular cofactors of hepatitis C virus replication. Cell Host Microbe 5: 298–307.
39. Vaillancourt FH, Pilote L, Cartier M, Lippens J, Liuzzi M, et al. (2009) Identification of a lipid kinase as a host factor involved in hepatitis C virus RNA replication. Virology 387: 5–10.
40. Amemiya F, Maekawa S, Itakura Y, Kanayama A, Matsui A, et al. (2008) Targeting lipid metabolism in the treatment of hepatitis C virus infection. J Infect Dis 197: 361–370.
41. Ishitsuka R, Sato SB, Kobayashi T (2005) Imaging lipid rafts. J Biochem 137: 249–254.
42. Ramstedt B, Slotte JP (2002) Membrane properties of sphingomyelins. FEBS Lett 531: 33–37.
43. He Q, Suzuki H, Sharma N, Sharma RP (2006) Ceramide synthase inhibition by fumonisin B1 treatment activates sphingolipid-metabolizing systems in mouse liver. Toxicol Sci 94: 388–397.
44. Bligh EG, Dyer WJ (1959) A rapid method of total lipid extraction and purification. Can J Biochem Physiol 37: 911–917.
45. Inoue K, Umehara T, Ruegg UT, Yasui F, Watanabe T, et al. (2007) Evaluation of a cyclophilin inhibitor in hepatitis C virus-infected chimeric mice in vivo. Hepatology 45: 921–928.
46. Kashiwakuma T, Hasegawa A, Kajita T, Takata A, Mori H, et al. (1996) Detection of hepatitis C virus specific core protein in serum of patients by a sensitive fluorescence enzyme immunoassay (FEIA). J Immunol Methods 190: 79–89.
47. Ikeda K, Shimizu T, Taguchi R (2008) Targeted analysis of ganglioside and sulfatide molecular species by LC/ESI-MS/MS with theoretically expanded multiple reaction monitoring. J Lipid Res 49: 2678–2689.
48. Taguchi R, Nishijima M, Shimizu T (2007) Basic analytical systems for lipidomics by mass spectrometry in Japan. Methods Enzymol 432: 185–211.
49. Ikeda K, Oike Y, Shimizu T, Taguchi R (2009) Global analysis of triacylglycerols including oxidized molecular species by reverse-phase high resolution LC/ESI-QTOF MS/MS. J Chromatogr B Analyt Technol Biomed Life Sci 877: 2639–2647.
50. Ikeda K, Mutoh M, Teraoka N, Nakanishi H, Wakabayashi K, et al. (2011) Increase of oxidant-related triglycerides and phosphatidylcholines in serum and small intestinal mucosa during development of intestinal polyp formation in Min mice. Cancer Sci 102: 79–87.

Virus Research 163 (2012) 390–395

Contents lists available at SciVerse ScienceDirect

Virus Research

journal homepage: www.elsevier.com/locate/virusres

Short communication

The interaction between human initiation factor eIF3 subunit c and heat-shock protein 90: A necessary factor for translation mediated by the hepatitis C virus internal ribosome entry site

Saneyuki Ujino[a], Hironori Nishitsuji[a], Ryuichi Sugiyama[a], Hitoshi Suzuki[a], Takayuki Hishiki[b], Kazuo Sugiyama[c], Kunitada Shimotohno[b], Hiroshi Takaku[a,*]

[a] Department of Life and Environmental Sciences, Chiba Institute of Technology, 2-17-1 Tsudanuma, Narashino-shi, Chiba 275-0016, Japan
[b] Research Institute, Chiba Institute of Technology, 2-17-1 Tsudanuma, Narashino, Chiba 275-0016, Japan
[c] Center for Integrated Medical Research, School of Medicine, Keio University, 35 Shinanomachi, Shinjyuku-ku Tokyo 160-8582, Japan

ARTICLE INFO

Article history:
Received 10 June 2011
Received in revised form 4 October 2011
Accepted 6 October 2011
Available online 14 October 2011

Keywords:
eIF3c
Hsp90
HCV IRES
17-AAG
Translation initiation

ABSTRACT

Heat-shock protein 90 (Hsp90) is a molecular chaperone that plays a key role in the conformational maturation of various transcription factors and protein kinases in signal transduction. The hepatitis C virus (HCV) internal ribosome entry site (IRES) RNA drives translation by directly recruiting the 40S ribosomal subunits that bind to eukaryotic initiation factor 3 (eIF3). Our data indicate that Hsp90 binds indirectly to eIF3 subunit c by interacting with it through the HCV IRES RNA, and the functional consequence of this Hsp90–eIF3c–HCV-IRES RNA interaction is the prevention of ubiquitination and the proteasome-dependent degradation of eIF3c. Hsp90 activity interference by Hsp90 inhibitors appears to be the result of the dissociation of eIF3c from Hsp90 in the presence of HCV IRES RNA and the resultant induction of the degradation of the free forms of eIF3c. Moreover, the interaction between Hsp90 and eIF3c is dependent on HCV IRES RNA binding. Furthermore, we demonstrate, by knockdown of eIF3c, that the silencing of eIF3c results in inhibitory effects on translation of HCV-derived RNA but does not affect cap-dependent translation. These results indicate that the interaction between Hsp90 and eIF3c may play an important role in HCV IRES-mediated translation.

The hepatitis C virus (HCV), a member of the *Flaviviridae* family, has a positive-strand RNA genome (Taylor et al., 1999; Bartenschlager and Lohmann, 2001) encoding a large precursor polyprotein that is cleaved by host and viral proteases to generate at least 10 functional viral proteins: core, envelope 1 (E1), E2, p7, nonstructural protein (NS2), NS3, NS4A, NS4B, NS5A, and NS5B (Grakoui et al., 1993; Hijikata et al., 1993). Ishii et al. identified an HCV replicon system in which the full HCV genomic RNA autonomously replicates in the Huh-7 human hepatoma cell line (Fig. 1A) (Ishii et al., 2006). This HCV replicon system allows researchers to study HCV genome replication in cell culture. HCV protein synthesis is initiated by the HCV RNA genome. This genome contains a conserved structure in its 5′-untranslated region (5′-UTR) that acts as an internal ribosome entry site (IRES) (Lukavsky, 2008). Briefly, the small ribosomal subunit (40S) and the eukaryotic initiation factor eIF3 bind specifically to the HCV IRES RNA, allowing for direct recognition of the start codon present in the 5′-UTR of the viral mRNA (Spahn et al., 2001; Collier et al., 2002; Kieft et al., 2002; Fraser and Doudna, 2007; Julien et al., 2009). Consistent with its diverse functions, eIF3 is the largest and most complex initiation factor. The mammalian version, for example, contains 13 nonidentical subunits designated eIF3a to eIF3m. The eIF3 core subunit (eIF3a–c, g, and i) is essential for translation (Kieft et al., 2002; Hinnebusch, 2006; Masutani et al., 2007; Zhou et al., 2008), and eIF3 specifically associates with the apical half of domain III of the HCV IRES (Kieft et al., 2001, 2002; Siridechadilok et al., 2005; Fraser and Doudna, 2007).

Hsp90 is a heat-shock protein that is abundant in the cytosol of eukaryotes and prokaryotes. In contrast to other chaperones, a number of substrates are known to contain Hsp90 (Schulte et al., 1995). Studies of eukaryotes have revealed that these Hsp90 client proteins include a variety of transcription factors (Coumailleau et al., 1995; Garcia-Cardena et al., 1998; Nagata et al., 1999; Sato et al., 2000; Richter and Buchner, 2001; Xu et al., 2001; Waza et al., 2005). Recently, many studies have reported that Hsp90 is involved with not only HCV RNA replication and viral protein but also HCV IRES-mediated translation (Waxman et al., 2001; Kim et al., 2006; Okamoto et al., 2006; Nakagawa et al., 2007; Ujino et al., 2009). In the present study, we demonstrate that eIF3 forms a complex with Hsp90 that is critical for HCV IRES-mediated translation.

* Corresponding author. Tel.: +81 47 478 0407; fax: +81 47 478 0407.
E-mail address: hiroshi.takaku@it-chiba.ac.jp (H. Takaku).

0168-1702/$ – see front matter © 2011 Elsevier B.V. All rights reserved.
doi:10.1016/j.virusres.2011.10.003

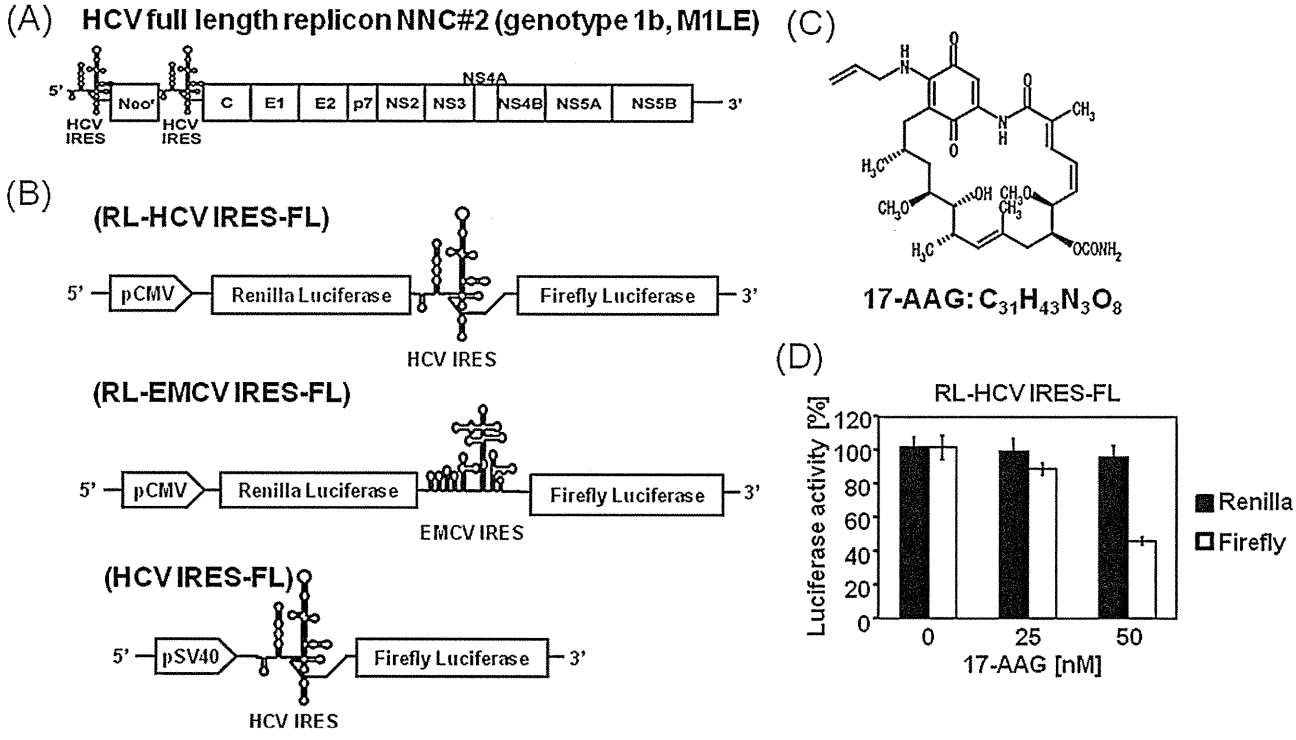

Fig. 1. Inhibition of IRES-mediated translation by an Hsp90 inhibitor. (A) The structure of the HCV replicon RNA molecules comprising the HCV 5′-UTR, including the HCV IRES, the neomycin phosphotransferase gene (Neo^r), and the coding region for the HCV proteins core to NS5B (in the HCV full-length replicon). (B) A schematic representation of the bicistronic HCV IRES or EMCV IRES reporter construct pRenilla-HCV IRES-firefly luciferase (RL-HCV IRES-FL) or pRenilla-EMCV IRES-firefly luciferase (RL-EMCV IRES-FL) driven by the CMV promoter to direct cap-dependent translation of renilla luciferase (RL) and HCV IRES or EMCV IRES-dependent translation of firefly luciferase (FL). The vector construct for HCV IRES-mediated translation of firefly luciferase, pHCV IRES-firefly luciferase (HCV IRES-FL) (Ujino et al., 2010). (C) The structure of the Hsp90 inhibitor 17-AAG (17-allylamino-17-demethoxygeldanamycin, Sigma–Aldrich Chemical Co.). (D) Inhibition of IRES-mediated translation by 17-AAG. Huh-7 cells (1×10^5 cells/well on 12-well plates) treated with 17-AAG (25 and 50 nM) and DMSO as a control for 24 h, and were then transfected with pRenilla-HCV IRES-firefly luciferase (RL-HCV IRES-FL) using Lipofectamine 2000 (Invitrogen). At 24 h post-transfection, Renilla luciferase (cap-dependent translation) and firefly luciferase (HCV IRES-dependent translation) activities were measured with a Dual-Luciferase Reporter Assay System (Promega). The data represent the mean ± standard deviations (SDs) from the experiments performed in triplicate.

To investigate the effects of the *Hsp90* inhibitor 17-AAG on HCV IRES translation, a bicistronic reporter system was used that consisted of an upstream reporter, Renilla luciferase (RL), expressed by cap-dependent translation and a downstream reporter, firefly luciferase (FL), which is under the translational control of the HCV IRES. To construct pcDNA-HCV IRES-firefly Luc, pHCV IRES-firefly Luc (HCV IRES-FL) (Ujino et al., 2010) (Fig. 1B) was digested with BamHI and SalI. The IRES-firefly Luc fragments were inserted into the BamHI-XhoI site of pcDNA3.1 (Invitrogen, Carlsbad, CA). To construct pRenilla-HCV IRES-firefly luciferase (RL-HCV IRES-FL), Renilla luciferase fragments were amplified by PCR from a pFN11A Flexi vector (Promega, Madison, WI), and the PCR products were inserted into the BamHI site of pcDNA-HCV IRES-firefly Luc. The human hepatoma cell line Huh-7 was maintained in Dulbecco's modified Eagle's medium (DMEM; Invitrogen) containing 10% fetal bovine serum (FBS). The benzoquinone ansamycin, the antibiotic geldanamycin (GA) and its less toxic analogue 17-allylamino-17-demethoxygeldanamycin (17-AAG) (Fig. 1C) (Sigma–Aldrich Chemical Co., St Louis, MO) directly bind to the ATP/ADP binding pocket of Hsp90, thus preventing ATP binding and the completion of client protein refolding (Neckers, 2003). The client proteins of Hsp90 appear to shift the role of the primary chaperone from Hsp90 to Hsp70 in cells treated with Hsp90 inhibitors (Doong et al., 2003). It is also well known that 17-AAG causes a modest increase in Hsp70 levels (Morimoto, 1998; Bagatell et al., 2000; Guo et al., 2005). In our previous report, a significant induction of Hsp70 was detected (Ujino et al., 2009).

For the reporter gene assay, Huh-7 cells were treated with different concentrations of the Hsp90 inhibitor, 17-AAG, or DMSO as a control for 24 h. They were then transfected with the bicistronic reporter construct RL-HCV IRES-FL using Lipofectamine 2000 (Invitrogen), which directs cap-dependent translation of the RL gene and HCV IRES-dependent translation of FL genes (Invitrogen). At 24 h post-transfection, the Renilla luciferase (cap-dependent translation) and firefly luciferase (HCV IRES-dependent translation) activities were measured with a Dual-Luciferase Reporter Assay System (Promega, Madison, WI). In cells treated with 50 nM 17-AAG, firefly luciferase activity was reduced by 55% with RL-HCV IRES-FL, whereas Renilla luciferase activity was mostly maintained (Fig. 1D). The inhibition of HCV IRES-mediated translation occurred in a dose-dependent manner. Recently, Kim et al. (2006) demonstrated that Hsp90 regulates ribosomal function by maintaining the stability of 40S ribosomal proteins such as rpS3 and rpS6. The interaction between the 40S ribosomal proteins and Hsp90 has also been associated with ribosomal activities such as protein synthesis. We also found that the Hsp90 inhibitor 17-AAG influences HCV IRES-mediated luciferase activity, suggesting that 17-AAG inhibited HCV RNA replication and HCV IRES-mediated translation.

The HCV IRES is recognized specifically by the small ribosomal subunit and eIF3 before the initiation of viral translation. Although the degradation of rpS3, a component of the small ribosomal subunit, has been shown to occur in the presence of the Hsp90 inhibitor (Kim et al., 2006), the influence of Hsp90 inhibition on eIF3 is not understood. To determine whether 17-AAG affects the expression of the eIF3 subunit, we analyzed eIF3a, eIF3b, eIF3c, eIF3g and eIF3i protein expression by western blot analysis. The HCV replicon cell line NNC#2 (NN/1b/FL), which carries a full genome replicon, was cultured in DMEM with 10% FBS, nonessential amino acids,

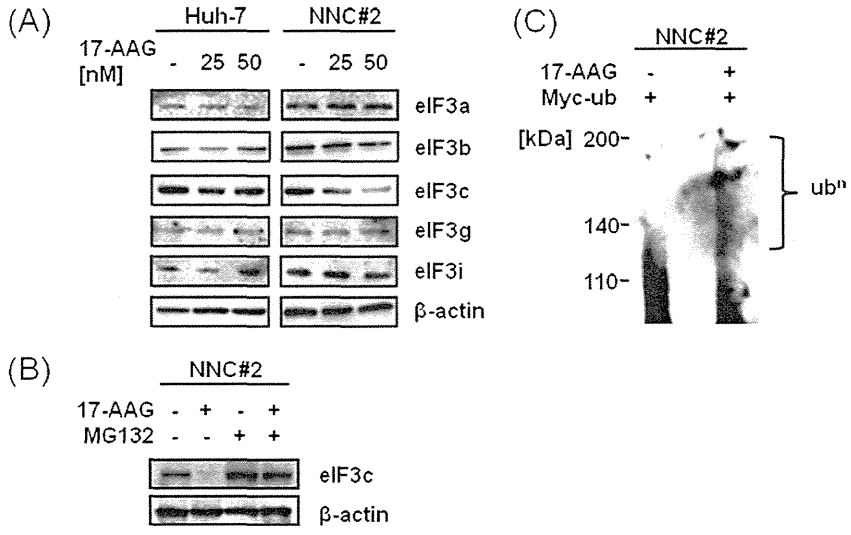

Fig. 2. Effect of 17-AAG treatment on eIF3 expression. (A) Western blot analysis of eIF3 protein expression in Huh-7 or NNC#2 cells treated with 17-AAG (25 nM and 50 nM). The cell lysates were analyzed by western blot 48 h after treatment. The primary antibodies used were monoclonal or polyclonal antibodies against eIF3a, eIF3b, eIF3c, eIF3g, and eIF3i (Santa Cruz Biotechnology). Horseradish peroxidase-conjugated anti-rabbit antibody (Sigma–Aldrich Chemical Co.) was used as the secondary antibody. (B) The reduction of eIF3c expression was prevented by proteasome inhibitor treatment. NNC#2 cells treated with 17-AAG (50 nM) or DMSO as a control. After 8 h treatment, the cells were treated with the proteasome inhibitor MG-132 (5 μM) or DMSO as a control. The cell lysates were analyzed by western blot 40 h after treatment. The primary antibody used was the eIF3c or β-actin (Santa Cruz Biotechnology). Horseradish peroxidase-conjugated anti-rabbit antibody (Sigma–Aldrich Chemical Co.) was used as the secondary antibody. (C) eIF3c degradation is mediated by the ubiquitin-dependent protease pathway. NNC#2 cells were transfected with pCMV-Myc-Ubi using Lipofectamine 2000 (Invitrogen). At 24 h post-transfection, the cells were treated with 17-AAG (50 nM) or DMSO as a control for 8 h and were then treated with the proteasome inhibitor MG-132 (5 μM) for 16 h. The cell lysates were subjected to an immunoprecipitation assay using an anti-αMyc antibody (Cell Signaling) followed by an immunoblot analysis using anti-eIF3c antibody.

L-glutamine, penicillin/streptomycin, and 1 mg/mL G418 (Invitrogen) at 37 °C in 5% CO_2 (Ishii et al., 2006). For western blot analysis, NNC#2 cells and Huh-7 cells were lysed in 1× chloramphenicol acetyltransferase (CAT) enzyme-linked immunosorbent assay buffer (Roche, Basel, Switzerland). The cell lysates were separated by 10% sodium dodecyl sulfate–polyacrylamide gel electrophoresis, transferred to nitrocellulose membranes, and blocked with 5% skimmed milk. The primary antibodies used were monoclonal or polyclonal antibodies against FLAG-M2 (Sigma–Aldrich Chemical Co.), Hsp90 (Cell Signaling Tech., Beverly, MA), eIF3a, eIF3b, eIF3c, eIF3g, and eIF3i (Santa Cruz Biotechnology, Santa Cruz, CA). Horseradish peroxidase-conjugated anti-rabbit antibody (Sigma–Aldrich Chemical Co.) was used as the secondary antibody. When the HCV replicon cell line NNC#2 (NN/1b/FL) and Huh-7 cells were treated with increasing doses of 17-AAG, the expression of the eIF3c subunit was markedly reduced in NNC#2 cells, but the expression in Huh-7 cells was unaffected (Fig. 2A). These results suggest that Hsp90 is involved in eIF3c stability through a physical interaction in the presence of HCV IRES RNA.

Protein degradation in cells is mediated by several protease systems; however, the stability of most proteins is regulated by Hsp90, and they appear to be degraded by proteasomes. To investigate whether the reduction of eIF3c was due to proteasomal degradation, we treated NNC#2 cells with a proteasome inhibitor, MG132, to prevent the 17-AAG-induced degradation of eIF3c. Our results indicated that 17-AAG-induced eIF3c degradation can be blocked by proteasome inhibitors (Fig. 2B). Proteasome inhibitors substantially prevented the degradation of eIF3c in cells treated with 17-AAG. This is most likely because the disruption of Hsp90 by the Hsp90 inhibitor treatment destabilized the eIF3c protein. Therefore, it is clear that proteasome-dependent degradation results in the decreased level of eIF3c protein. This indicates that the stability of eIF3c was supported by Hsp90, and unstable eIF3c was removed by proteasomes. Furthermore, we investigated whether the ubiquitination of eIF3c was affected by the Hsp90 inhibitor, 17-AAG. We transfected pCMV-Myc-Ubi (provided by Dr. A. Ryo) using Lipofectamine 2000 (Invitrogen) into NNC#2 cells, which were then treated with 17-AAG (50 μM). After treatment, the cells were then treated with 5 μM MG132 and subjected to immunoprecipitation with an anti-αMyc antibody (Cell Signaling) followed by an immunoblot analysis using an anti-eIF3c antibody. Notably, polyubiquitinated forms of eiF3c was detected in cells treated with 17-AAG (Fig. 2C). These results suggest that the destabilized eIF3c protein is degraded by proteasome-dependent proteolysis mediated by ubiquitin conjugation, and Hsp90 plays an important role in maintaining the stable form of the eIF3c protein in vivo.

To investigate the influence of eIF3c silencing on HCV IRES-mediated translation, Huh-7 cells were transfected with siRNA targeted to eIF3c at a concentration of 50 nM using Lipofectamine 2000 (Invitrogen), and they were then transfected with RL-HCV IRES-FL. Control small interference RNA (siRNA) and eIF3 p110 (eukaryotic translation initiation factor 3, subunit 8, 110 kDa) siRNA were purchased from Santa Cruz Biotechnology. The protein levels of eIF3c were examined by western blot analysis, and HCV IRES-mediated translation was analyzed with a Dual-Luciferase Assay. As demonstrated in Fig. 3A, when compared to Huh-7 cells treated with control siRNA, the eIF3c protein level was markedly reduced in Huh-7 cells transfected with eIF3 p110 siRNA targeting eIF3c. Furthermore, firefly luciferase activity in RL-HCV IRES-FL was also reduced by approximately 63% in the cells treated with siRNA targeted to eIF3c, whereas Renilla luciferase activity was mostly maintained (Fig. 3B). The inhibition of HCV IRES-mediated translation by siRNA against eIF3c indicates that the suppression of HCV IRES-mediated translation by Hsp90 inhibition leads to a reduction in eIF3c. To further characterize the HCV IRES inhibitory effect of siRNA targeting eIF3c, we used additional bicistronic reporter plasmids for transient transfection assays with Huh-7 cells. Since we were mainly interested in viral IRESs, we chose to investigate the effect of the luciferase activities on translation derived from the IRES of EMCV in place of the HCV IRES (Fig. 1B). To generate pcDNA-EMCV IRES-firefly Luc, EMCV IRES fragments were created by PCR using the following primers: 5′-GAC TGG ATC CCC CCC CCT AAC-3′ and 5′-CAG TGG GCC CTA TTA TCG TGT TTT TCA AAG GAA AAC C-3′. The PCR products were inserted into the BamHI and

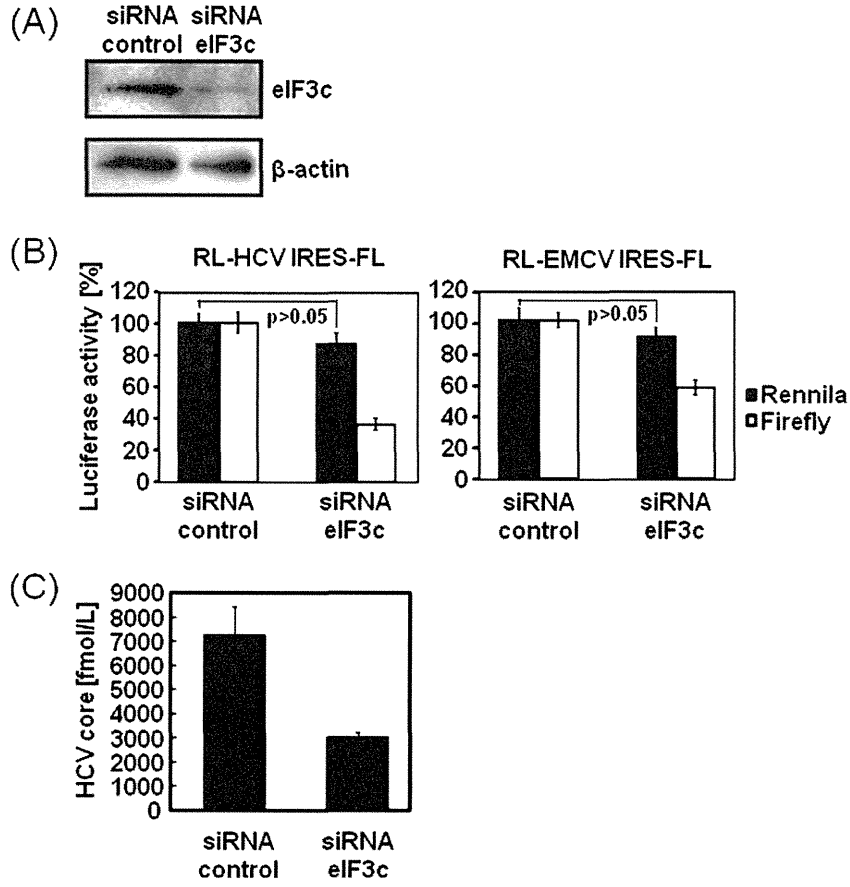

Fig. 3. Knockdown of eIF3c expression inhibits HCV IRES-mediated translation. (A) eIF3c protein expression in Huh-7 cells transfected with control siRNA or eIF3c siRNA at a concentration of 50 nM using Lipofectamine 2000 (Invitrogen). Cell lysates were analyzed by western blot 24 h post-treatment. eIF3c or β-actin antibodies were used as the primary antibodies (Santa Cruz Biotechnology). Horseradish peroxidase-conjugated anti-rabbit antibody (Sigma–Aldrich Chemical Co.) was used as the secondary antibody. (B) Huh-7 cells were transfected with siRNA targeted to eIF3c (50 nM) or nontarget control siRNA (50 nM) using Lipofectamine 2000 (Invitrogen). At 24 h post-transfection, the cells were then transfected with RL-HCV IRES-FL or RL-EMCV IRES-FL using Lipofectamine 2000 (Invitrogen). At 24 h post-transfection, the Renilla luciferase (cap-dependent translation) and firefly luciferase (HCV IRES or EMCV IRES-dependent translation) activities were measured with a Dual-Luciferase Reporter Assay System (Promega). Results are representative of three independent experiments, and error bars indicate the ± standard deviations (SDs) of the means. $P > 0.05$ (Student's t-test). (C) HCV IRES-mediated translational inhibition with eIF3 p110 siRNA by HCV full-genome RNA (NN/1b/FL). Huh-7 cells were transfected with eIF3 p110 siRNA or control siRNA at a concentration of 50 nM using Lipofectamine 2000 (Invitrogen). At 24 h post-transfection, the cells were transfected with 2 μg of HCV full-genome RNA (NN/1b/FL) using Lipofectamine 2000 (Invitrogen). After 24 h, intracellular HCV core-protein levels were measured using a fully automated HCV core-protein antigen chemiluminescent enzyme immunoassay (CLEIA) according to the manufacturer's instructions (Aoyagi et al., 1999). The relative chemiluminescence units were measured and used to determine the concentration of the HCV core antigen according to a standard curve generated using recombinant HCV core antigen. The concentration was expressed in units of femtomole/L (fmol/L). The data represent the mean ± standard deviations (SDs) from the experiments performed in triplicate.

ApaI sites of pcDNA3.1, and firefly Luc fragments were cloned into the ApaI site of the resulting plasmid. To construct pcDNA-Renilla-EMCV IRES-firefly Luc (RL-EMCV IRES-FL), pcDNA-Renilla-EMCV IRES-firefly Luc was digested with BamHI, and the renilla Luc fragments were inserted into BamHI site of pcDNA-EMCV IRES-firefly Luc (Fig. 1B). Huh-7 cells were transfected with control small interference RNA (siRNA) or eIF3 p110 siRNA at a concentration of 50 nM using Lipofectamine 2000 (Invitrogen) and then transfected with RL-EMCV IRES-FL. Following transient transfection in Huh-7 cells, firefly luciferase activity in RL-EMCV IRES-FL was also reduced by approximately 43% in cells treated with siRNA targeting eIF3c, but Renilla luciferase activity was mostly maintained (Fig. 3B). The knockdown of eIF3c expression also resulted in inhibitory effects on translation derived from HCV and EMCV (Fig. 3B) but did not affect cap-dependent translation. These results indicate that eIF3c may play a more important initiation factor in IRES-mediated translation than cap-dependent translation. However, it remains the subject of future investigation to determine whether only eIF3c proteins are subject to the IRES-mediated translation.

We also examined the HCV IRES-mediated translational inhibition with eIF3 p110 siRNA by HCV full-genome RNA ((NN/1b/FL) (Ishii et al., 2006). Huh-7 cells were transfected with eIF3 p110 siRNA or control siRNA at a concentration of 50 nM using Lipofectamine 2000 (Invitrogen). At 24 h post-transfection, the cells were transfected with HCV full-genome RNA (NN/1b/FL). After 24 h, the intracellular HCV core-protein levels were measured using a fully automated HCV core-protein antigen chemiluminescent enzyme immunoassay (CLEIA) according to the manufacturer's instructions (Aoyagi et al., 1999). The core-protein expression in cells treated with eIF3 p110 siRNA was reduced by approximately 61% when compared to cells treated with control siRNA (Fig. 3C). These findings further confirmed that HCV IRES-mediated translational inhibition occurs through a reduction of eIF3c expression caused by the Hsp90 inhibitor-mediated disruption of the interaction between eIF3c and Hsp90 with HCV IRES RNA.

To investigate the role of Hsp90 in HCV IRES-mediated translation further, we confirmed the interaction of eIF3c and Hsp90 by immunoprecipitation. The pFLAG-eIF3c vector was constructed by subcloning a DNA fragment encoding full-length human eiF3c into the EcoRI and XbaI sites of the pFLAG CMV^{TM}-2 expression vector (Sigma–Aldrich Chemical Co.) so that the amino-terminal FLAG epitope was fused in-frame with eIF3c. The pFLAG-eIF3c expression vector or the control vector pFLAG-CMV2 was transfected into NNC#2 cells or Huh-7 cells. After 48 h, the immunoprecipitates

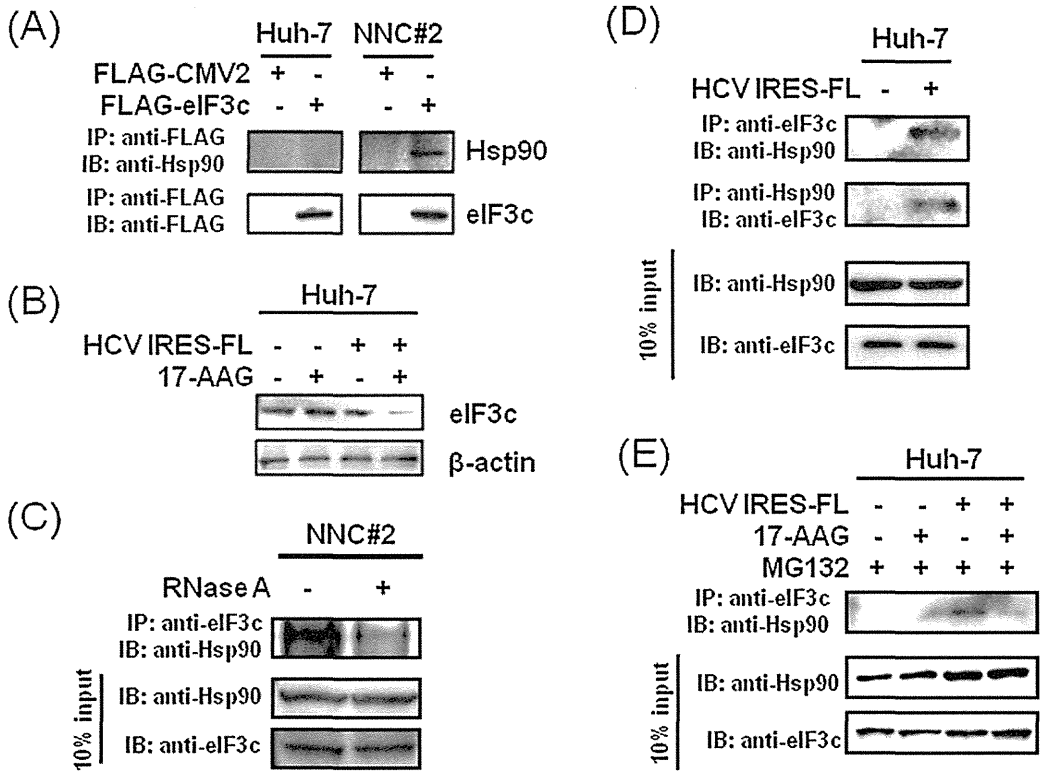

Fig. 4. An interaction between eIF3c and Hsp90 was induced by HCV IRES. (A) The pFLAG-eIF3c vector was constructed by subcloning a DNA fragment encoding full-length human eiF3c into the EcoRI and XbaI sites of the pFLAG CMV™-2 expression vector (Sigma–Aldrich Chemical Co.) such that the amino-terminal FLAG epitope was fused in-frame with eIF3c. Huh-7 and NNC#2 cells were transfected with pFLAG-eIF3c or pFLAG-CMV2 control plasmids using Lipofectamine 2000 (Invitrogen). Cell lysates were immunoprecipitated by the anti-FLAG M2 antibody 48 h after transfection. The precipitates were analyzed by western blot using the anti-Hsp90 antibody. (B) The Huh-7 cells were transfected with or without pHCV IRES-firefly luciferase (HCV IRES-FL) (Fig. 1B) and then treated with or without 17-AAG (50 nM). Cell lysates were analyzed by western blot 48 h post-treatment with an eIF3c primary antibody (Santa Cruz Biotechnology). Horseradish peroxidase-conjugated anti-rabbit antibody (Sigma-Aldrich Chemical Co.) was used as the secondary antibody. β-Actin was used as an internal control. (C) The interruption of Hsp90–eIF3c interaction by RNase A treatment. NNC#2 cell lysates were treated with RNase A (5 U/μL) (Sigma–Aldrich Chemical Co.). After 4 h, the cell lysates were subjected to immunoprecipitation using an anti-eIF3c antibody, followed by immunoblot analysis using an anti-Hsp90 antibody. (D) eIF3c or Hsp90 co-immunoprecipitates with Hsp90 or eIF3c from cells transfected or untransfected with pHCV IRES-FL. Huh-7 cells were transfected with pHCV IRES-FL using Lipofectamine 2000 (Invitrogen) and subject to immunoprecipitation using the indicated antibodies at 24 h post-transfection. The precipitates were analyzed by western blot using the indicated antibodies. (E) The inhibitor 17-AAG dissociates Hsp90 and eIF3c from the HCV IRES complex. Huh-7 cells were transfected with pHCV IRES-FL using Lipofectamine 2000 (Invitrogen). At 24 h post-transfection, cells were treated with 17-AAG (50 nM) or DMSO as a control for 8 h and were then treated with MG132 (5 μM) for 16 h. Cell lysates were subjected to immunoprecipitation using an anti-eIF3c antibody, and the precipitates were analyzed by western blot using the anti-Hsp90 antibody.

(anti-FLAG antibody) were determined by western blot analysis (Fig. 4A). The western blot analysis clearly indicated that eIF3c and Hsp90 coprecipitated in NNC#2 cells, whereas they did not coprecipitate in Huh-7 cells, suggesting that eIF3c was bound to the chaperone complex that formed with Hsp90 in NNC#2 cells (Fig. 4A). This interaction between Hsp90 and eIF3c in NNC#2 cells suggests that HCV translation is due to the interaction between eIF3c and Hsp90. Given the observed binding of eIF3 with the HCV IRES RNA, this Hsp90-eIF3c interaction occurring in HCV replicon cells was likely mediated by HCV IRES RNA. To address this question, Huh-7 cells were transfected with pHCV IRES-firefly luciferase (HCV IRES-FL) (Fig. 1B) using Lipofectamine 2000 (Invitrogen) and then treated with 17-AAG (50 nM) or DMSO as a control. After treatment, the cell lysates were analyzed by western blot (Fig. 4B). The level of eIF3c was reduced by the 17-AAG treatment in cells transfected with pHCV IRES-FL compared to control DMSO, but eIF3c was not reduced in cells transfected with pHCV IRES-FL. The disruption of Hsp90 activity by the Hsp90 inhibitor, 17-AAG, appears to dissociate eIF3c from the Hsp90-eIF3c-HCV IRES complex and induce the degradation of the free forms of eIF3c. To verify this result, NNC#2 cell lysates were further treated with RNase A (5 U/μL) (Sigma–Aldrich Chemical Co.). After treatment, anti-eIF3c antibody immunoprecipitates were determined by western blot analysis (Fig. 4C). The analysis clearly indicated that eIF3c and Hsp90 coprecipitated in NNC#2 cell lysates, whereas they did not coprecipitate in NNC#2 cells lysates treated with RNase A. The interaction between Hsp90 and eIF3c was interrupted by RNase A treatment. These results suggest that the interaction of eIF3c and Hsp90 is dependent on HCV IRES binding. Next, to further demonstrate whether HCV IRES is required for the interaction between eIF3c and Hsp90, we performed a co-immunoprecipitation assay using the extracts of cells transfected with pHCV IRES-FL. eIF3c co-immunoprecipitated with anti-Hsp90 (Fig. 4D). The interaction of eIF3c and Hsp90 was further confirmed by reverse co-immunoprecipitation of Hsp90 and eIF3c (Fig. 4D). These results also indicated that the interaction of eIF3c and Hsp90 was supported by the HCV IRES. Furthermore, we performed an immunoprecipitation assay to confirm that eIF3c and Hsp90 interaction was influenced by the treatment with 17-AAG in cells transfected with pHCV IRES-FL. Huh-7 cells were transfected with pHCV IRES-FL using Lipofectamine 2000 (Invitrogen). At 24 h post-transfection, the cells were treated with 17-AAG (50 nM) or DMSO as a control for 8 h and then MG132 (5 μM) for 16 h. An immunoprecipitation assay with the cell lysates was performed using the anti-eIF3c antibody, and the precipitates were analyzed by western blot using the anti-Hsp90 antibody. Although treatment with both 17-AAG and MG132 in cells transfected with pHCV IRES-FL resulted in a reduction in the interaction of Hsp90 and eIF3c, eIF3c expression recovered upon treatment with the proteasome inhibitor MG132 (Fig. 4E), but the interaction between

Hsp90 and eIF3c was not restored (Fig. 4E). Furthermore, eIF3c was not detected in cells not treated with MG132 (Fig. 2B), which indicates that eIF3c is a client protein for active Hsp90 (Fig. 2C). In contrast, an interaction between Hsp90 and eIF3c was observed in cells not treated with 17-AAG (Fig. 4E). These results suggest that the interaction between Hsp90 and eIF3c is specific to HCV IRES-expressing cells. However, the interaction of Hsp90 and eIF3c in the presence of 17-AAG, which blocks the association of Hsp90 with eIF3c, may dissociate Hsp90 and eIF3c from the overall HCV IRES complex (Figs. 2B and C, and 4B and E).

In conclusion, our results demonstrate that HCV IRES-mediated translational inhibition occurs through a reduction of eIF3c expression caused by the Hsp90 inhibitor-mediated disruption of the interaction between eIF3c and Hsp90 with HCV IRES RNA. Furthermore, the interaction between Hsp90 and eIF3c requires HCV IRES RNA. Taken together, our results suggest that the interaction between Hsp90 and eIF3c plays an important role in HCV IRES-mediated translation. More experiments are needed to verify the relationship between eukaryotic initiation factor 3 (eIF3) and Hsp90.

Conflict of interest

The authors declare no conflict of interest.

Acknowledgements

We thank Dr. A. Ryo for providing pCMV-Myc-Ubi. We are grateful to S. Yamaguchi, M. Sato, and Y. Katumura for their excellent technical assistance. This work was supported by a Grant-in-Aid for HCV Research from the Ministry of Health, Labor, and Welfare of Japan, by a Grant-in-Aid for High Technology Research (HTR) from the Ministry of Education, Science, Sports, and Culture of Japan, and a Grant from the Strategic Research Foundation Grant-aided Project for Private Universities from the Ministry of Education, Culture, Sport, Science, and Technology, Japan (MEXT).

References

Aoyagi, K., Ohue, C., Iida, K., Kimura, T., Tanaka, E., Kiyosawa, K., Yagi, S., 1999. Development of a simple and highly sensitive enzyme immunoassay for hepatitis C virus core antigen. J. Clin. Microbiol. 37 (6), 1802–1808.

Bagatell, R., Paine-Murrieta, G.D., Taylor, C.W., Pulcini, E.J., Akinaga, S., Benjamin, J., Whitesell, L., 2000. Induction of a heat shock factor 1-dependent stress response alters the cytotoxic activity of hsp90-binding agents. Clin. Cancer Res. 6 (8), 3312–3318.

Bartenschlager, R., Lohmann, V., 2001. Novel cell culture systems for the hepatitis C virus. Antivir. Res. 52 (1), 1–17.

Collier, A.J., Gallego, J., Klinck, R., Cole, P.T., Harris, S.J., Harrison, G.P., Aboul-Ela, F., Varani, G., Walker, S., 2002. A conserved RNA structure within the HCV IRES eiF3-binding site. Nat. Struct. Biol. 9 (5), 375–380.

Coumailleau, P., Poellinger, L., Gustafsson, J.A., Whitelaw, M.L., 1995. Definition of a minimal domain of the dioxin receptor that is associated with Hsp90 and maintains wild type ligand binding affinity and specificity. J. Biol. Chem. 270 (42), 25291–25300.

Doong, H., Rizzo, K., Fang, S., Kulpa, V., Weissman, A.M., Kohn, E.C., 2003. CAIR-1/BAG-3 abrogates heat shock protein-70 chaperone complex-mediated protein degradation: accumulation of poly-ubiquitinated Hsp90 client proteins. J. Biol. Chem. 278 (31), 28490–28500.

Fraser, C.S., Doudna, J.A., 2007. Structural and mechanistic insights into hepatitis C viral translation initiation. Nat. Rev. Microbiol. 5 (1), 29–38.

Garcia-Cardena, G., Fan, R., Shah, V., Sorrentino, R., Cirino, G., Papapetropoulos, A., Sessa, W.C., 1998. Dynamic activation of endothelial nitric oxide synthase by Hsp90. Nature 392, 821–824.

Grakoui, A., Wychowski, C., Lin, C., Feinstone, S.M., Rice, C.M., 1993. Expression and identification of hepatitis C virus polyprotein cleavage products. J. Virol. 67 (3), 1385–1395.

Guo, F., Rocha, K., Bali, P., Pranpat, M., Fiskus, W., Boyapalle, S., Kumaraswamy, S., Balasis, M., Greedy, B., Armitage, E.S., Lawrence, N., Bhalla, K., 2005. Abrogation of heat shock protein 70 induction as a strategy to increase antileukemia activity of heat shock protein 90 inhibitor 17-allylamino-demethoxy geldanamycin. Cancer Res. 65 (22), 10536–10544.

Hijikata, M., Mizushima, H., Shimotohno, K., 1993. Two distinct proteinase activities required for the processing of a putative nonstructural precursor protein of hepatitis C virus. J. Virol. 67 (8), 4665–4675.

Hinnebusch, A.G., 2006. eIF3: a versatile scaffold for translation initiation complexes. Trends Biochem. Sci. 10, 553–562.

Ishii, N., Watashi, K., Hishiki, T., Goto, K., Inoue, D., Hijikata, M., Wakita, T., Kato, N., Shimotohno, K., 2006. Diverse effects of cyclosporine on hepatitis C virus strain replication. J. Virol. 80 (9), 4510–4520.

Julien, P., Rodolfo, R., Jan, M., Isabel, A., Jerome, B., Emmanuel, D., Florence, B., 2009. Human initiation factor eIF3 subunit b interacts with HCV IRES RNA through its N-terminal RNA recognition motif. FEBS Lett. 583 (1), 70–74.

Kieft, J.S., Zhou, K., Jubin, R., Doudna, J.A., 2001. Mechanism of ribosome recruitment by hepatitis C IRES RNA. RNA 7 (2), 194–206.

Kieft, J.S., Zhou, K., Grech, A., Jubin, R., Doudna, J.A., 2002. Crystal structure of an RNA tertiary domain essential to HCV IRES-mediated translation initiation. Nat. Struct. Biol. 9 (5), 370–374.

Kim, T.S., Jang, K., Kim, C.-Y., Lee, H.D., Ahn, J.Y., Kim, B.-Y., 2006. J. Interaction of Hsp90 with ribosomal proteins protects from ubiquitination and proteasome-dependent degradation. Mol. Biol. Cell 17 (2), 824–833.

Lukavsky, P.J., 2008. Structure and function of HCV IRES domains. Virus Res. 139 (2), 166–171.

Masutani, M., Sonenberg, N., Yokoyama, S., Imataka, H., 2007. Reconstitution reveals the functional core of mammalian eIF3. EMBO J. 26 (14), 3373–3383.

Morimoto, R.I., 1998. Regulation of the heat shock transcriptional response: cross talk between a family of heat shock factors, molecular chaperones, and negative regulators. Genes Dev. 12 (24), 3788–3796.

Nagata, Y., Anan, T., Yoshida, T., Mizukami, T., Taya, Y., Fujiwara, T., Kato, H., Saya, H., Nakao, M., 1999. The stabilization mechanism of mutant-type p53 by impaired ubiquitination: the loss of wild-type p53 function and the hsp90 association. Oncogene 18 (44), 6037–6049.

Neckers, L., 2003. Development of small molecule Hsp90 inhibitors: utilizing both forward and reverse chemical genomics for drug identification. Curr. Med. Chem. 10 (9), 733–739.

Nakagawa, S., Umehara, T., Matsuda, C., Kuge, S., Sudoh, M., Kohara, M., 2007. Hsp90 inhibitors suppress HCV replication in replicon cells and humanized liver mice. Biochem. Biophys. Res. Commun. 353 (4), 882–888.

Okamoto, T., Nishimura, Y., Ichimura, T., Suzuki, K., Miyamura, T., Suzuki, T., Moriishi, K., Matsuura, Y., 2006. hepatitis C virus RNA replication is regulated by FKBP8 and Hsp90. EMBO J. 25 (20), 5015–5025.

Richter, K., Buchner, J., 2001. Hsp90, chaperoning signal transduction. J. Cell. Physiol. 188 (3), 281–290.

Sato, S., Fujita, N., Tsuruo, T., 2000. Modulation of Akt kinase activity by binding to Hsp90. Proc. Natl. Acad. Sci. U.S.A. 97 (20), 10832–10837.

Schulte, T.W., Blagosklonny, M.V., Ingui, C., Neckers, L., 1995. Disruption of the Raf-1-Hsp90 molecular complex results in destabilization of Raf-1 and loss of Raf-1-Ras association. J. Biol. Chem. 270 (41), 24585–24588.

Siridechadilok, B., Fraser, C.S., Hall, R.J., Doudna, J.A., Nogales, E., 2005. Structural roles for human translation factor eIF3 in initiation of protein synthesis. Science 310, 1513–1515.

Spahn, C.M., Kieft, J.S., Grassucci, R.A., Penczek, P.A., Zhou, K., Doudna, J.A., Frank, J., 2001. Hepatitis C virus IRES RNA-induced changes in the conformation of the 40s ribosomal subunit. Science 291, 1959–1962.

Taylor, D.R., Shi, S.T., Tomano, P.R., Barber, G.N., Lai, M.M., 1999. Inhibition of the interferon-inducible protein kinase PKR by HCV E2 protein. Science 285, 107–110.

Ujino, S., Yamaguchi, S., Shimotohno, K., Takaku, H., 2009. Heat-shock protein 90 is essential for stabilization of the hepatitis C virus nonstructural protein NS3. J. Biol. Chem. 284 (11), 6841–6846.

Ujino, S., Yamaguchi, S., Shimotohno, K., Takaku, H., 2010. Combination therapy for hepatitis C virus with heat-shock protein 90 inhibitor 17-AAG and proteasome inhibitor MG132. Antivir. Chem. Chemother. 20 (4), 161–167.

Waxman, L., Whitney, M., Pollok, B.A., Kuo, L.C., Darke, P.L., 2001. Host cell factor requirement for hepatitis C virus enzyme maturation. Proc. Natl. Acad. Sci. U.S.A. 98 (24), 13931–13935.

Waza, M., Adachi, H., Katsuno, M., Minamiyama, M., Sang, C., Tanaka, F., Inukai, A., Doyu, M., Sobue, G., 2005. 17-AAG, an Hsp90 inhibitor, ameliorates polyglutamine-mediated motor neuron degeneration. Nat. Med. 11 (10), 1088–1095.

Xu, W., Mimnaugh, E., Rosser, M.F., Nicchitta, C., Marcu, M., Yarden, Y., Neckers, L., 2001. Sensitivity of mature Erbb2 to geldanamycin is conferred by its kinase domain and is mediated by the chaperone protein Hsp90. J. Biol. Chem. 276 (5), 3702–3708.

Zhou, M., Sandercock, A.M., Fraser, C.S., Ridlova, G., Stephens, E., Schenauer, M.R., Yokoi-Fong, T., Barsky, D., Leary, J.A., Hershey, J.W., Doudna, J.A., Robinson, C.V., 2008. Mass spectrometry reveals modularity and a complete subunit interaction map of the eukaryotic translation factor eIF3. Proc. Natl. Acad. Sci. U.S.A. 105 (47), 18139–18144.

frontiers in
MICROBIOLOGY

MINI REVIEW ARTICLE
published: 10 January 2012
doi: 10.3389/fmicb.2011.00278

Molecular mechanism of hepatitis C virus-induced glucose metabolic disorders

Ikuo Shoji*, Lin Deng and Hak Hotta

Division of Microbiology, Center for Infectious Diseases, Kobe University Graduate School of Medicine, Kobe, Japan

Edited by:
Yasuko Yokota, National Institute of Infectious Diseases, Japan

Reviewed by:
Koji Ishii, National Institute of Infectious Diseases, Japan
Kohji Moriishi, University of Yamanashi, Japan

****Correspondence:***
Ikuo Shoji, Division of Microbiology, Center for Infectious Diseases, Kobe University Graduate School of Medicine, 7-5-1 Kusunoki-cho, Chuo-ku, Kobe, Hyogo 650-0017, Japan.
e-mail: ishoji@med.kobe-u.ac.jp

Hepatitis C virus (HCV) infection causes not only intrahepatic diseases but also extrahepatic manifestations, including metabolic disorders. Chronic HCV infection is often associated with type 2 diabetes. However, the precise mechanism underlying this association is still unclear. Glucose is transported into hepatocytes via glucose transporter 2 (GLUT2). Hepatocytes play a crucial role in maintaining plasma glucose homeostasis via the gluconeogenic and glycolytic pathways. We have been investigating the molecular mechanism of HCV-related type 2 diabetes using HCV RNA replicon cells and HCV J6/JFH1 system. We found that HCV replication down-regulates cell surface expression of GLUT2 at the transcriptional level. We also found that HCV infection promotes hepatic gluconeogenesis in HCV J6/JFH1-infected Huh-7.5 cells. HCV infection transcriptionally up-regulated the genes for phosphoenolpyruvate carboxykinase (PEPCK) and glucose 6-phosphatase (G6Pase), the rate-limiting enzymes for hepatic gluconeogenesis. Gene expression of PEPCK and G6Pase was regulated by the transcription factor forkhead box O1 (FoxO1) in HCV-infected cells. Phosphorylation of FoxO1 at Ser319 was markedly diminished in HCV-infected cells, resulting in increased nuclear accumulation of FoxO1. HCV NS5A protein was directly linked with the FoxO1-dependent increased gluconeogenesis. This paper will discuss the current model of HCV-induced glucose metabolic disorders.

Keywords: HCV, diabetes, gluconeogenesis, GLUT2, FoxO1, JNK, NS5A

INTRODUCTION

Hepatitis C virus (HCV) is a positive-sense, single stranded RNA virus that belongs to the genus *Hepacivirus* of the family *Flaviviridae*. The approximately 9.6-kb HCV genome encodes a unique open reading frame that is translated into a polyprotein of about 3,000 amino acids, which is cleaved by cellular signalases and viral proteases to generate at least 10 viral proteins, such as core, envelope 1 (E1) and E2, p7, NS2, NS3, NS4A, NS4B, NS5A, and NS5B (Choo et al., 1991; Lemon et al., 2007).

Hepatitis C virus is the main cause of chronic hepatitis, liver cirrhosis, and hepatocellular carcinoma. More than 170 million people worldwide are chronically infected with HCV (Poynard et al., 2003). Persistent HCV infection causes not only liver diseases but also extrahepatic manifestations. It is well established that HCV perturbs the glucose metabolism, leading to insulin resistance and type 2 diabetes in predisposed individuals. Several epidemiological, clinical, and experimental data suggested that HCV infection serves as an additional risk factor for the development of diabetes (Mason et al., 1999; Negro and Alaei, 2009; Negro, 2011). HCV-related glucose metabolic changes and insulin resistance and diabetes have significant clinical consequences, such as accelerated fibrogenesis, increased incidence of hepatocellular carcinoma, and reduced virological response to interferon (IFN)-α-based therapy (Negro, 2011). Therefore, it is very important to clarify the molecular mechanism of HCV-related diabetes. However, the precise mechanisms are poorly understood.

Experimental data suggest a direct interference of HCV with the insulin signaling pathway. Transgenic mice expressing HCV core gene exhibit insulin resistance (Shintani et al., 2004; Koike, 2007). In this transgenic mice model, both tyrosine phosphorylation of the insulin receptor substrate (IRS)-1 and IRS-2 are decreased. These decreases are recovered when the proteasome activator PA28γ is deleted, suggesting that the HCV core protein suppresses insulin signaling through a PA28γ-dependent pathway (Miyamoto et al., 2007). Several other reports also showed a link of the HCV core protein with insulin resistance (Kawaguchi et al., 2004; Pazienza et al., 2007).

Hepatocytes play a crucial role in maintaining plasma glucose homeostasis by adjusting the balance between hepatic glucose production and utilization via the gluconeogenic and glycolytic pathways, respectively. Gluconeogenesis is mainly regulated at the transcriptional level of the glucose 6-phosphatase (G6Pase) and phosphoenolpyruvate carboxykinase (PEPCK) genes, whereas glycolysis is mainly regulated by glucokinase (GK). Gluconeogenesis and glycolysis are coordinated so that one pathway is highly active within a cell while the other is relatively inactive. It is well known that increased hepatic glucose production via gluconeogenesis is a major feature of type 2 diabetes (Clore et al., 2000).

To identify a novel mechanism of HCV-related diabetes, we have been investigating the effects of HCV on glucose production in hepatocytes using HCV RNA replicon cells (Lohmann et al., 1999) and HCV J6/JFH1 cell culture system (Lindenbach et al., 2005; Wakita et al., 2005; Bungyoku et al., 2009). We previously reported that HCV replication suppresses cellular glucose uptake through down-regulation of cell surface expression of glucose transporter 2 (GLUT2; Kasai et al., 2009). Furthermore, we

recently reported that HCV promotes hepatic gluconeogenesis via an NS5A-mediated, forkhead box O1 (FoxO1)-dependent pathway, resulting in increased cellular glucose production in hepatocytes (Deng et al., 2011). This paper discusses our current model for HCV-induced glucose metabolic disorders.

HCV REPLICATION DOWN-REGULATES CELL SURFACE EXPRESSION OF GLUT2

The uptake of glucose into cells is conducted by the facilitative glucose carrier, glucose transporters (GLUTs). GLUTs are integral membrane proteins that contain 12 membrane-spanning helices. To date, a total of 14 isoforms have been identified in the GLUT family (Wu and Freeze, 2002; Macheda et al., 2005; Godoy et al., 2006). Glucose is transported into hepatocytes by GLUT2. We previously reported that HCV J6/JFH1 infection suppresses hepatocytic glucose uptake through down-regulation of surface expression of GLUT2 in human hepatoma cell line, Huh-7.5 cells (Kasai et al., 2009). We also demonstrated that GLUT2 expression in hepatocytes of the liver tissues from HCV-infected patients was significantly lower than in those from patients without HCV infection. Our data suggest that HCV infection down-regulates GLUT2 expression at transcriptional level. We are currently analyzing transcriptional control of human GLUT2 promoter in HCV replicon cells as well as in HCV J6/JFH1-infected cells.

HCV INFECTION PROMOTES HEPATIC GLUCONEOGENESIS

Then we analyzed hepatic glucose production and expression of transcription factors using HCV replicon cells and HCVcc system in order to clarify a role of HCV infection in glucose metabolic changes. Hepatic glucose production is usually regulated by gluconeogenesis and glycolysis. Therefore, we examined whether HCV infection induces gluconeogenesis or glycolysis. We found that the PEPCK and G6Pase genes were transcriptionally up-regulated in J6/JFH1-infected cells (**Figure 1**). On the other hand, the GK gene was transcriptionally down-regulated in HCV-infected cells. We obtained similar data in HCV replicon cells (both in subgenomic replicon cells and full-genomic replicon cells). When HCV replication was suppressed by IFN treatment, the up-regulation of PEPCK and G6Pase gene expression as well as the down-regulation of GK gene expression were canceled. From these results, HCV infection selectively up-regulates PEPCK and G6Pase genes, whereas HCV infection down-regulates GK gene (Deng et al., 2011).

Both HCV replicon cells and HCV-infected cells produced greater amounts of glucose than the control cells. IFN treatment canceled the enhanced glucose production in HCV replicon cells as well as in HCV-infected cells. G6P is an important precursor molecule that is converted to glucose in the gluconeogenesis pathway (**Figure 1**). Our metabolite analysis showed that a significantly higher level of G6P was accumulated in HCV-infected cells than in the control cells, suggesting that HCV indeed promotes hepatic gluconeogenesis to cause hyperglycemia. There is a trend toward an increase in gluconeogenesis in HCV-infected cells (**Figure 1**).

HCV SUPPRESSES FoxO1 PHOSPHORYLATION AT Ser319, LEADING TO THE NUCLEAR ACCUMULATION OF FoxO1

It has been reported that G6Pase, PEPCK, and GK are regulated by certain transcription factors, including FoxO1 (Hirota et al., 2008), hepatic nuclear factor 4α (HNF-4α; Hirota et al.,

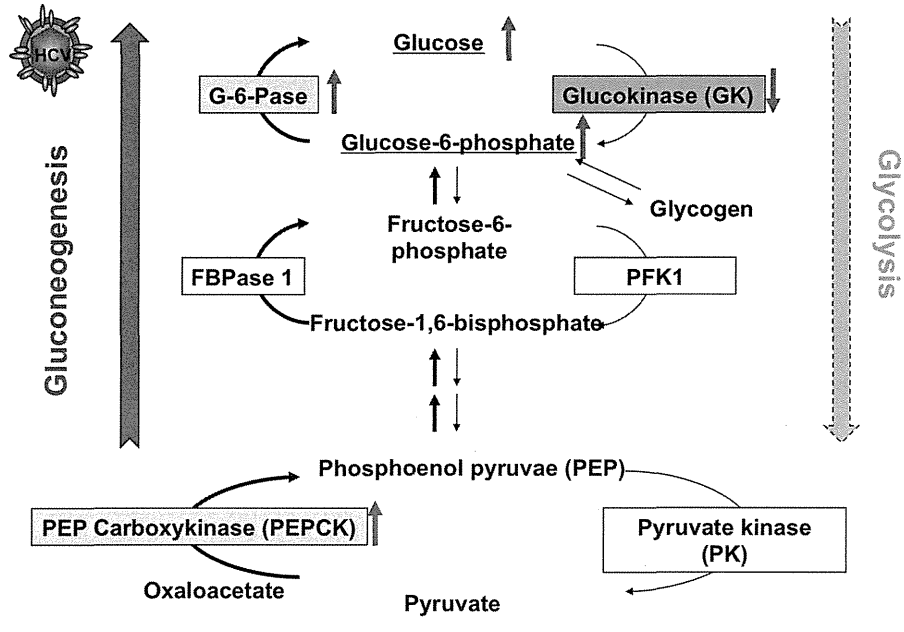

FIGURE 1 | Regulation of Gluconeogenesis and Glycolysis in the HCV-infected cells. HCV infection promotes gluconeogenesis via transcriptional up-regulation of the genes for PEPCK and G6Pase, the rate-limiting enzymes for hepatic gluconeogenesis, and transcriptional down-regulation of the gene for GK, the rate-limiting enzyme for hepatic glycolysis.

2008), Krüppel-like factor 15 (KLF15; Takashima et al., 2010), and cyclic AMP (cAMP) response element binding protein (CREB; Rozance et al., 2008). While we were analyzing these factors in both HCV replicon cells and HCV J6/JFH1-infected cells, we found the involvement of the FoxO1 in the transcriptional activation of G6Pase and PEPCK (Deng et al., 2011). It is known that the FoxO1 enhances gluconeogenesis through the transcriptional activation of various genes, including G6Pase and PEPCK (Gross et al., 2008). The function of FoxO1 is regulated by post-translational modifications, including phosphorylation, ubiquitylation, and acetylation (Tzivion et al., 2011). The phosphorylated form of FoxO1 is exported from the nucleus to the cytosol, resulting in loss of its transcriptional activity (**Figure 2**). Phosphorylation status of FoxO1 at Ser319 is critical for FoxO1 nuclear exclusion (Zhao et al., 2004). Although the total amounts of FoxO1 protein were unchanged, FoxO1 phosphorylation at Ser319 was markedly suppressed in HCV-infected cells compared to that in the mock-infected cells. It is known that the FoxO1 is phosphorylated by the protein kinase Akt and is exported from the nucleus to the cytosol, resulting in loss of its transcriptional activity (Tzivion et al., 2011). The majority of FoxO1 was accumulated in the nuclear fraction in HCV-infected cells, whereas in control cells FoxO1 was distributed in both the nuclear and cytoplasmic fractions. Akt phosphorylation was enhanced in HCV-infected cells, although the protein levels of total Akt protein were comparable, which is consistent with the report by Burdette et al. (2010). Our findings suggest an interesting scenario in which the HCV-mediated suppression in FoxO1 phosphorylation is caused by an unknown mechanism independent of Akt activity.

HCV-INDUCED JNK ACTIVATION IS INVOLVED IN THE SUPPRESSION OF FoxO1 PHOSPHORYLATION

It is known that the stress-sensitive serine/threonine kinase JNK regulates FoxO at multiple levels (van der Horst and Burgering, 2007; Karpac and Jasper, 2009). We demonstrated that HCV infection induces phosphorylation and activation of JNK in a time-dependent manner, which is similar to that observed for the suppression of FoxO1 phosphorylation. As a result, c-Jun, a key substrate for JNK, got phosphorylated and activated in HCV-infected cells. The JNK inhibitor SP600125 clearly prevented the phosphorylation of c-Jun, and concomitantly recovered the suppression of FoxO1 phosphorylation in HCV-infected cells, suggesting that HCV activates the JNK/c-Jun signaling pathway, resulting in the nuclear accumulation of FoxO1 by reducing its phosphorylation status. The detailed mechanisms of HCV-induced suppression of FoxO1 phosphorylation via the JNK/c-Jun signaling pathway remain to be explored. There are at least two possibilities. The JNK/c-Jun signaling pathway (1) suppresses a protein kinase, or (2) activates a protein phosphatase to reduce phosphorylation of FoxO1.

HCV-INDUCED MITOCHONDRIAL REACTIVE OXYGEN SPECIES PRODUCTION IS INVOLVED IN INCREASED GLUCOSE PRODUCTION THROUGH JNK ACTIVATION

Hepatitis C virus infection increases mitochondrial reactive oxygen species (ROS) production (Deng et al., 2008). *N*-acetyl cysteine (NAC; a general antioxidant) clearly prevented the phosphorylation of JNK, and concomitantly canceled the suppression of FoxO1 phosphorylation in HCV-infected cells, suggesting that

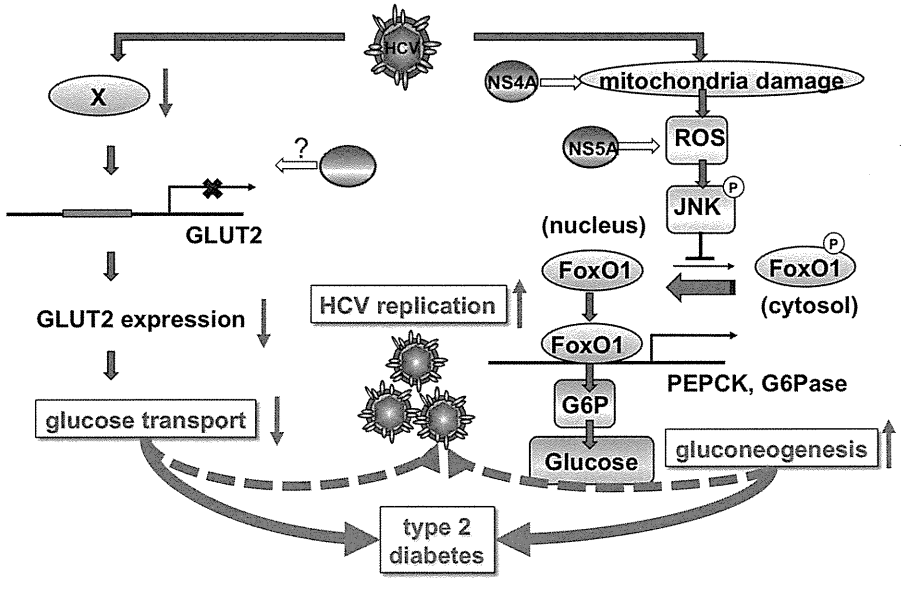

FIGURE 2 | A proposed mechanism of HCV-induced glucose metabolic disorders. HCV infection down-regulates cell surface expression of GLUT2 in hepatocytes at the transcriptional level. HCV down-regulates a transcription factor involved in GLUT2 gene expression through an unknown mechanism. HCV infection induces mitochondria damage and ROS production, leading to JNK activation. HCV NS4A protein is involved in mitochondrial damage. HCV NS5A protein is involved in ROS production. HCV-induced ROS production causes JNK activation, resulting in the decreased phosphorylation and nuclear accumulation of FoxO1. Nuclear accumulation of FoxO1 up-regulates gene expression of PEPCK and G6Pase, leading eventually to increased glucose production by gluconeogenesis. High glucose levels in the hepatocytes may confer an advantage in efficient replication of HCV.

HCV-induced ROS production is involved in the JNK activation. There was no significant difference in HCV RNA replication or infectious virus release between SP600125- or NAC-treated HCV-infected cells and non-treated HCV-infected cells. These results suggest that ROS-mediated JNK activation plays a key role in the suppression of FoxO1 phosphorylation, nuclear accumulation of FoxO1, and enhancement of glucose production in HCV-infected cells (Deng et al., 2011).

HCV NS5A IS INVOLVED IN THE ENHANCEMENT OF GLUCOSE PRODUCTION

Then we sought to determine which HCV protein(s) is involved in the enhancement of glucose production. Transient expression of NS5A protein in Huh-7.5 cells significantly promoted the gene expression levels of G6Pase and PEPCK determined by real time quantitative RT-PCR. Promoter assay revealed that the level of PEPCK promoter activity was significantly higher in NS5A-expressing cells than in the control cells. Our results suggest that NS5A activate both the PEPCK promoter and the G6Pase promoter, leading to an increase in glucose production (Deng et al., 2011). The study by Banerjee et al. (2010) suggests that the HCV core protein modulates FoxO1 and FoxA2 activation and affects insulin-induced metabolic gene regulation in human hepatocytes. Our results, however, suggest that the HCV core protein is not significantly involved in the increased gluconeogenesis (Deng et al., 2011). The difference between these two studies needs to be explored.

There were previous reports suggesting that ROS production is induced in NS5A-expressing cells (Dionisio et al., 2009) or in hepatocytes of NS5A transgenic mice (Wang et al., 2009). We therefore sought to determine whether NS5A contributes to increased hepatic gluconeogenesis through the induction of ROS production. NS5A-expressing cells displayed a much stronger signal of ROS than in control cells. NS5A-expressing cells promoted phosphorylation level at Ser63 of c-Jun and suppressed FoxO1 phosphorylation at Ser319, suggesting that NS5A mediates JNK/c-Jun activation and FoxO1 phosphorylation suppression. These results suggest that NS5A play a role in the HCV-induced enhancement of hepatic gluconeogenesis through JNK/c-Jun activation and FoxO1 phosphorylation suppression.

CONCLUSION AND FUTURE PERSPECTIVES

Taken together, we propose a model of HCV-induced glucose metabolic disorders as shown in **Figure 2**. HCV infection down-regulates cell surface expression of GLUT2 in hepatocytes at the transcriptional level. HCV down-regulates a transcription factor involved in GLUT2 gene expression through an unknown mechanism. As GLUT2 is a facilitative GLUT, it ensures large bidirectional fluxes of glucose in and out the cell due to its low affinity and high capacity (Leturque et al., 2009). Down-regulated cell surface expression of GLUT2 results in disruption of bidirectional transport of glucose in hepatocytes. Even in the fasting state, down-regulation of GLUT2 may result in low glucose uptake of hepatocytes, causing hyperglycemia. In the fed state, glucose secretion from hepatocytes may be suppressed due to low level cell surface expression of GLUT2, as GLUT2 is a bidirectional transporter.

Hepatitis C virus infection induces mitochondria damage and ROS production, leading to JNK activation. HCV NS4A protein is involved in mitochondrial damage (Nomura-Takigawa et al., 2006). HCV NS5A protein is involved in ROS production (Dionisio et al., 2009; Wang et al., 2009; Deng et al., 2011). HCV-induced ROS production causes JNK activation, which results in the decreased phosphorylation and nuclear accumulation of FoxO1 by an unidentified mechanism. Nuclear accumulation of FoxO1 up-regulates gene expression of PEPCK and G6Pase, leading eventually to increased glucose production by gluconeogenesis (Deng et al., 2011).

These two pathways, HCV-induced down-regulation of GLUT2 expression and up-regulation of gluconeogenesis, may contribute to development of type 2 diabetes in HCV-infected patients at least to some extent. HCV-induced down-regulation of GLUT2 expression and up-regulation of gluconeogenesis may result in high concentration of glucose in HCV-infected hepatocytes. As suggested in a recent study, low glucose concentration in the hepatocytes inhibits HCV replication (Nakashima et al., 2011). Therefore, high glucose levels in the hepatocytes may confer an advantage in efficient replication of HCV.

Our understanding of HCV-induced glucose metabolic disorders will require much more work to fully unfold this pathway. Further investigation including the mechanism of HCV-induced GLUT2 downregualtion, JNK-mediated decreased phosphorylation of FoxO1, and the possible effect(s) of the dysregulation of hepatic gluconeogenesis on the HCV life cycle and host cells are currently under way.

ACKNOWLEDGMENTS

The authors are grateful to all of their co-workers who contributed to the studies cited here. This work was supported in part by grants-in-aid for Research on Hepatitis from the Ministry of Health, Labor and Welfare, Japan, and the Japan Initiative for Global Research Network on Infectious Diseases (J-GRID) program of Ministry of Education, Culture, Sports, Science and Technology, Japan. This study was also carried out as part of the Global Center of Excellence program of Kobe University Graduate School of Medicine, and the Science and Technology Research Partnership for Sustainable Development (SATREPS) program of Japan Science and Technology Agency (JST) and Japan International Cooperation Agency (JICA).

REFERENCES

Banerjee, A., Meyer, K., Mazumdar, B., Ray, R. B., and Ray, R. (2010). Hepatitis C virus differentially modulates activation of forkhead transcription factors and insulin-induced metabolic gene expression. *J. Virol.* 84, 5936–5946.

Bungyoku, Y., Shoji, I., Makine, T., Adachi, T., Hayashida, K., Nagano-Fujii, M., Ide, Y. H., Deng, L., and Hotta, H. (2009). Efficient production of infectious hepatitis C virus with adaptive mutations in cultured hepatoma cells. *J. Gen. Virol.* 90, 1681–1691.

Burdette, D., Olivarez, M., and Waris, G. (2010). Activation of transcription factor Nrf2 by hepatitis C virus induces the cell-survival pathway. *J. Gen. Virol.* 91, 681–690.

Choo, Q. L., Richman, K. H., Han, J. H., Berger, K., Lee, C., Dong, C., Gallegos, C., Coit, D., Medina-Selby,

R., Barr, P. J., Weiner, A. J., Bradley, D. W., Kuo, G., and Houghton, M. (1991). Genetic organization and diversity of the hepatitis C virus. *Proc. Natl. Acad. Sci. U.S.A.* 88, 2451–2455.

Clore, J. N., Stillman, J., and Sugerman, H. (2000). Glucose-6-phosphatase flux in vitro is increased in type 2 diabetes. *Diabetes* 49, 969–974.

Deng, L., Adachi, T., Kitayama, K., Bungyoku, Y., Kitazawa, S., Ishido, S., Shoji, I., and Hotta, H. (2008). Hepatitis C virus infection induces apoptosis through a Bax-triggered, mitochondrion-mediated, caspase 3-dependent pathway. *J. Virol.* 82, 10375–10385.

Deng, L., Shoji, I., Ogawa, W., Kaneda, S., Soga, T., Jiang, D. P., Ide, Y. H., and Hotta, H. (2011). Hepatitis C virus infection promotes hepatic gluconeogenesis through an NS5A-mediated, FoxO1-dependent pathway. *J. Virol.* 85, 8556–8568.

Dionisio, N., Garcia-Mediavilla, M. V., Sanchez-Campos, S., Majano, P. L., Benedicto, I., Rosado, J. A., Salido, G. M., and Gonzalez-Gallego, J. (2009). Hepatitis C virus NS5A and core proteins induce oxidative stress-mediated calcium signalling alterations in hepatocytes. *J. Hepatol.* 50, 872–882.

Godoy, A., Ulloa, V., Rodriguez, F., Reinicke, K., Yanez, A. J., Garcia Mde, L., Medina, R. A., Carrasco, M., Barberis, S., Castro, T., Martinez, F., Koch, X., Vera, J. C., Poblete, M. T., Figueroa, C. D., Peruzzo, B., Perez, F., and Nualart, F. (2006). Differential subcellular distribution of glucose transporters GLUT1-6 and GLUT9 in human cancer: ultrastructural localization of GLUT1 and GLUT5 in breast tumor tissues. *J. Cell. Physiol.* 207, 614–627.

Gross, D. N., van den Heuvel, A. P., and Birnbaum, M. J. (2008). The role of FoxO in the regulation of metabolism. *Oncogene* 27, 2320–2336.

Hirota, K., Sakamaki, J., Ishida, J., Shimamoto, Y., Nishihara, S., Kodama, N., Ohta, K., Yamamoto, M., Tanimoto, K., and Fukamizu, A. (2008). A combination of HNF-4 and Foxo1 is required for reciprocal transcriptional regulation of glucokinase and glucose-6-phosphatase genes in response to fasting and feeding. *J. Biol. Chem.* 283, 32432–32441.

Karpac, J., and Jasper, H. (2009). Insulin and JNK: optimizing metabolic homeostasis and lifespan. *Trends Endocrinol. Metab.* 20, 100–106.

Kasai, D., Adachi, T., Deng, L., Nagano-Fujii, M., Sada, K., Ikeda, M., Kato, N., Ide, Y. H., Shoji, I., and Hotta, H. (2009). HCV replication suppresses cellular glucose uptake through down-regulation of cell surface expression of glucose transporters. *J. Hepatol.* 50, 883–894.

Kawaguchi, T., Yoshida, T., Harada, M., Hisamoto, T., Nagao, Y., Ide, T., Taniguchi, E., Kumemura, H., Hanada, S., Maeyama, M., Baba, S., Koga, H., Kumashiro, R., Ueno, T., Ogata, H., Yoshimura, A., and Sata, M. (2004). Hepatitis C virus down-regulates insulin receptor substrates 1 and 2 through up-regulation of suppressor of cytokine signaling 3. *Am. J. Pathol.* 165, 1499–1508.

Koike, K. (2007). Hepatitis C virus contributes to hepatocarcinogenesis by modulating metabolic and intracellular signaling pathways. *J. Gastroenterol. Hepatol.* 22(Suppl. 1), S108–S111.

Lemon, S. M., Walker, C., Alter, M. J., and Yi, M. (2007). "Hepatitis C virus," in *Fields' Virology*, 5th Edn, eds B. N. Fields, D. M. Knipe, and P. M. Howley (Philadelphia, PA: Wolters Kluwer Health/Lippincott Williams and Wilkins), 1291–1304.

Leturque, A., Brot-Laroche, E., and Le Gall, M. (2009). GLUT2 mutations, translocation, and receptor function in diet sugar managing. *Am. J. Physiol. Endocrinol. Metab.* 296, E985–E992.

Lindenbach, B. D., Evans, M. J., Syder, A. J., Wolk, B., Tellinghuisen, T. L., Liu, C. C., Maruyama, T., Hynes, R. O., Burton, D. R., McKeating, J. A., and Rice, C. M. (2005). Complete replication of hepatitis C virus in cell culture. *Science* 309, 623–626.

Lohmann, V., Korner, F., Koch, J., Herian, U., Theilmann, L., and Bartenschlager, R. (1999). Replication of subgenomic hepatitis C virus RNAs in a hepatoma cell line. *Science* 285, 110–113.

Macheda, M. L., Rogers, S., and Best, J. D. (2005). Molecular and cellular regulation of glucose transporter (GLUT) proteins in cancer. *J. Cell. Physiol.* 202, 654–662.

Mason, A. L., Lau, J. Y., Hoang, N., Qian, K., Alexander, G. J., Xu, L., Guo, L., Jacob, S., Regenstein, F. G., Zimmerman, R., Everhart, J. E., Wasserfall, C., Maclaren, N. K., and Perrillo, R. P. (1999). Association of diabetes mellitus and chronic hepatitis C virus infection. *Hepatology* 29, 328–333.

Miyamoto, H., Moriishi, K., Moriya, K., Murata, S., Tanaka, K., Suzuki, T., Miyamura, T., Koike, K., and Matsuura, Y. (2007). Involvement of the PA28gamma-dependent pathway in insulin resistance induced by hepatitis C virus core protein. *J. Virol.* 81, 1727–1735.

Nakashima, K., Takeuchi, K., Chihara, K., Hotta, H., and Sada, K. (2011). Inhibition of hepatitis C virus replication through adenosine monophosphate-activated protein kinase-dependent and -independent pathways. *Microbiol. Immunol.* 55, 774–782.

Negro, F. (2011). Mechanisms of hepatitis C virus-related insulin resistance. *Clin. Res. Hepatol. Gastroenterol.* 35, 358–363.

Negro, F., and Alaei, M. (2009). Hepatitis C virus and type 2 diabetes. *World J. Gastroenterol.* 15, 1537–1547.

Nomura-Takigawa, Y., Nagano-Fujii, M., Deng, L., Kitazawa, S., Ishido, S., Sada, K., and Hotta, H. (2006). Non-structural protein 4A of Hepatitis C virus accumulates on mitochondria and renders the cells prone to undergoing mitochondria-mediated apoptosis. *J. Gen. Virol.* 87, 1935–1945.

Pazienza, V., Clement, S., Pugnale, P., Conzelman, S., Foti, M., Mangia, A., and Negro, F. (2007). The hepatitis C virus core protein of genotypes 3a and 1b downregulates insulin receptor substrate 1 through genotype-specific mechanisms. *Hepatology* 45, 1164–1171.

Poynard, T., Yuen, M. F., Ratziu, V., and Lai, C. L. (2003). Viral hepatitis C. *Lancet* 362, 2095–2100.

Rozance, P. J., Limesand, S. W., Barry, J. S., Brown, L. D., Thorn, S. R., LoTurco, D., Regnault, T. R., Friedman, J. E. and Hay, W. W. Jr. (2008). Chronic late-gestation hypoglycemia upregulates hepatic PEPCK associated with increased PGC1alpha mRNA and phosphorylated CREB in fetal sheep. *Am. J. Physiol. Endocrinol. Metab.* 294, E365–E370.

Shintani, Y., Fujie, H., Miyoshi, H., Tsutsumi, T., Tsukamoto, K., Kimura, S., Moriya, K., and Koike, K. (2004). Hepatitis C virus infection and diabetes: direct involvement of the virus in the development of insulin resistance. *Gastroenterology* 126, 840–848.

Takashima, M., Ogawa, W., Hayashi, K., Inoue, H., Kinoshita, S., Okamoto, Y., Sakaue, H., Wataoka, Y., Emi, A., Senga, Y., Matsuki, Y., Watanabe, E., Hiramatsu, R., and Kasuga, M. (2010). Role of KLF15 in regulation of hepatic gluconeogenesis and metformin action. *Diabetes* 59, 1608–1615.

Tzivion, G., Dobson, M., and Ramakrishnan, G. (2011). FoxO transcription factors; Regulation by AKT and 14-3-3 proteins. *Biochim. Biophys. Acta* 1813, 1938–1945.

van der Horst, A., and Burgering, B. M. (2007). Stressing the role of FoxO proteins in lifespan and disease. *Nat. Rev. Mol. Cell Biol.* 8, 440–450.

Wakita, T., Pietschmann, T., Kato, T., Date, T., Miyamoto, M., Zhao, Z., Murthy, K., Habermann, A., Krausslich, H. G., Mizokami, M., Bartenschlager, R., and Liang, T. J. (2005). Production of infectious hepatitis C virus in tissue culture from a cloned viral genome. *Nat. Med.* 11, 791–796.

Wang, A. G., Lee, D. S., Moon, H. B., Kim, J. M., Cho, K. H., Choi, S. H., Ha, H. L., Han, Y. H., Kim, D. G., Hwang, S. B., and Yu, D. Y. (2009). Non-structural 5A protein of hepatitis C virus induces a range of liver pathology in transgenic mice. *J. Pathol.* 219, 253–262.

Wu, X., and Freeze, H. H. (2002). GLUT14, a duplicon of GLUT3, is specifically expressed in testis as alternative splice forms. *Genomics* 80, 553–557.

Zhao, X., Gan, L., Pan, H., Kan, D., Majeski, M., Adam, S. A., and Unterman, T. G. (2004). Multiple elements regulate nuclear/cytoplasmic shuttling of FOXO1: characterization of phosphorylation- and 14-3-3-dependent and -independent mechanisms. *Biochem. J.* 378, 839–849.

Conflict of Interest Statement: The authors declare that the research was conducted in the absence of any commercial or financial relationships that could be construed as a potential conflict of interest.

Received: 01 December 2011; accepted: 25 December 2011; published online: 10 January 2012.

Citation: Shoji I, Deng L and Hotta H (2012) Molecular mechanism of hepatitis C virus-induced glucose metabolic disorders. Front. Microbio. 2:278. doi: 10.3389/fmicb.2011.00278

This article was submitted to Frontiers in Virology, a specialty of Frontiers in Microbiology.

ELSEVIER

Institut Pasteur

Microbes and Infection 14 (2012) 69–78

www.elsevier.com/locate/micinf

Original article

Generation of a recombinant reporter hepatitis C virus useful for the analyses of virus entry, intra-cellular replication and virion production

Kazuya Kamada [a], Ikuo Shoji [a], Lin Deng [a], Chie Aoki [a,b], Suratno Lulut Ratnoglik [a,b], Takaji Wakita [c], Hak Hotta [a,b,*]

[a] *Division of Microbiology, Kobe University, Graduate School of Medicine, 7-5-1 Kusunoki-cho, Cyuo-ku, Kobe, Hyogo 650-0017, Japan*
[b] *JST/JICA SATREPS, Japan*
[c] *Department of Virology II, National Institute of Infectious Diseases, Shinjuku-ku, Tokyo 162-8640, Japan*

Received 21 February 2011; accepted 18 August 2011
Available online 31 August 2011

Abstract

The lack of a culture system that efficiently produces progeny virus has hampered hepatitis C virus (HCV) research. Recently, the discovery of a novel HCV isolate JFH1 and its chimeric derivative J6/JFH1 has led to the development of an efficient virus productive culture system. To construct an easy monitoring system for the viral life cycle of HCV, we generated bicistronic luciferase reporter virus genomes based on the JFH1 and J6/JFH1 isolates, respectively. Transfection of the J6/JFH1-based reporter genome to Huh7.5 cells produced significantly greater levels of progeny virus than transfection of the JFH1 genome. Furthermore, the expression of dominant-negative Vps4, a key molecule of the endosomal sorting complex required for transport machinery, inhibited the virus production of JFH1, but not that of J6/JFH1. These results may account for the different abilities to produce progeny virus between JFH1 and J6/JFH1. Using the J6/JFH1/Luc system, we showed that the two polyanions heparin and polyvinyl sulfate decreased the infectivity of J6/JFH1/Luc virus in a dose-dependent manner. We also analyzed the function of microRNA on HCV replication and found that miR-34b could affect the replication of HCV. The reporter virus generated in this study will be useful for investigating the nature of the HCV life cycle and for identification of HCV inhibitors.

Keywords: HCV; Reporter virus; Virus production; ESCRT; microRNA

1. Introduction

Hepatitis C virus (HCV) is an enveloped virus and has a positive-stranded RNA genome of about 9.6 kb [1,2]. HCV persistently infects hepatocytes, and the persistent infection can lead to liver cirrhosis and hepatocellular carcinoma. Considering that approximately 170 million people are infected with HCV worldwide [3], HCV is a major public health problem throughout the world. A combination therapy of pegylated interferon-α and ribavirin has been established as the standard of care for treating HCV infection [3,4]. Nonetheless, approximately 50% of individuals with chronic HCV infection are still unable to resolve infection [4,5]. For this reason, more effective therapies are greatly needed against the disease caused by HCV infection [6].

The HCV genome encodes a 3000 amino acid polyprotein which is cleaved by host and viral proteases to yield the mature structural proteins, composed of core and glycoprotein E1 and E2, and the non-structural proteins p7, NS2, NS3, NS4A, NS4B, NS5A, and NS5B [1–3]. Translation of the HCV open reading frames is mediated via the 5′ untranslated region and a part of the core coding region carrying the internal ribosome entry site (IRES) [1,7].

In 1999, Bartenschlager and his colleagues produced the HCV replicon system, a tissue culture system that recapitulated the RNA replication of HCV in a human hepatoma cell line [8]. In the initial subgenomic replicon system, genes

* Corresponding author. Division of Microbiology, Kobe University, Graduate School of Medicine, 7-5-1 Kusunoki-cho, Cyuo-ku, Kobe, Hyogo 650-0017, Japan. Tel.: +81 78 382 5500; fax: +81 78 382 5519.
E-mail address: hotta@kobe-u.ac.jp (H. Hotta).

1286-4579/$ - see front matter © 2011 Institut Pasteur. Published by Elsevier Masson SAS. All rights reserved.
doi:10.1016/j.micinf.2011.08.009

unessential for RNA replication that contained the core, E1, E2, p7 and NS2 of the HCV genome were replaced with a genetic cassette carrying an antibiotics resistance gene and IRES from encephalomyocarditis virus (EMCV). The development of a subgenomic replicon system became a driving force for the studies on the mechanism of HCV replication, and these studies revealed numerous biological features of HCV replication. However, the resulting systems were unable to produce progeny virus. Therefore, the nature of the HCV, i.e., the virus production and virus entry, remained unclear for a long while.

Wakita and his colleagues isolated a full-length HCV genome from the sera of a patient with fulminant hepatitis [9]. The HCV strain, designated JFH1, belongs to genotype 2a. The transfection of the Huh7 hepatoma cell line with the JFH1 genome yields a progeny virus called HCVcc that is infectious both *in vivo* and *in vitro*. The HCVcc system allowed us to perform virological studies to investigate the nature of HCV [9,10]. However, the analyses using HCVcc have not been suitable for carrying out high-throughput screening due to the labor-intensive quantitative reverse transcription-PCR methods used in screening and the difficulties presented by the low signal-to-noise ratios.

In this study, to develop a robust tool for use in the screening of HCV replication, we have constructed a genome-length luciferase reporter HCV derived from the JFH1 and J6/JFH1 strains, and used it to analyze the intra-cellular RNA replication and extra-cellular progeny virus production. We demonstrated here that our recombinant reporter HCV system was useful for studying viral genome replication, virus entry, and virion production of HCV.

2. Materials and methods

2.1. Plasmids

The plasmid pFGR-JFH1/Luc, which encodes bicistronic constructs of HCV IRES-driven firefly luciferase reporter genes and the EMCV IRES-driven full-genomic JFH1 genome, was constructed by insertion of the JFH1 full genome of pJFH1 [9] into pSGR-JFH1 [11]. The plasmid pFL-J6/JFH1, which contains a chimeric full-genome composed of the 5′NCR to NS2 region derived from J6 and NS3 to the 3′NCR region from JFH1 [10], was kindly supplied by C.M. Rice of the Center for the Study of Hepatitis C, Rockefeller University. To yield the bicistronic luciferase reporter construct composed of full-length J6/JFH1, the JFH1 full genome of pFGR-JFH1/Luc was replaced with the J6/JFH1 full genome of pFL-J6/JFH1 by digestion with BstZ17I, and the resultant plasmid was designated as pFGR-J6/JFH1/Luc. As a negative control for the HCV replication, a non-synonymous mutation at NS5B (GDD to GND), which disrupts NS5B polymerase activity, was introduced into the pFGR-J6/JFH1/Luc NS5B region by site-directed mutagenesis, and the resultant plasmid was designated pFGR-J6/JFH1/Luc (GND).

2.2. Cell culture and indirect immunofluorescence

All experiments described in this study were performed by using Huh7.5 human hepatoma cells, a highly HCV-susceptible subclone of Huh7 cells. The cells were cultured in Dulbecco's minimum essential medium (DMEM) supplemented with 10% heat-inactivated fetal bovine serum, 2 mM glutamine, and 0.01% streptomycin, and were subcultured twice weekly. Huh7.5 cells electroporated with JFH1/Luc or J6/JFH1/Luc RNA were subjected to indirect immunofluorescence analysis as previously reported [12]. The primary antibody used was derived from an HCV-infected patient's serum. The secondary antibody used was fluorescein isothiocyanate (FITC)-conjugated goat anti-human IgG (MBL, Nagoya, Japan).

2.3. In vitro transcription and electroporation

Plasmid DNA was linearized with XbaI, extracted with phenol and chloroform, precipitated with ethanol, and dissolved in RNase-free water. The purified DNA was used for *in vitro* RNA transcription using a T7 Megascript kit (Ambion, Austin, TX) following the manufacturer's protocols. The concentration was determined by measurement of the optical density at 260 nm, and the RNA integrity was checked by agarose gel electrophoresis. The *in vitro*-transcribed RNA (10 μg) was transfected into Huh7.5 cells by means of electroporation (975 μF, 270 V) using a Gene Pulser (Bio-Rad, Hercules, CA). The cells were then cultured in complete medium. The culture fluid of transfected cells was harvested and cleared by passing through 0.45-μm-pore-size filters and stored at −80 °C until use.

2.4. Luciferase assay

The *firefly* luciferase activity was measured by a luciferase assay system (Promega, Madison, WS). The cells were harvested, washed twice with dication-free phosphate buffered saline (PBS), and lysed in a passive lysis buffer supplied by the manufacturer. A 20-μl sample of the lysate was subjected to a luciferase assay. The luminescence was measured at 10 s after an initial 2 s delay according to the manufacturer's instructions, using a Lumat LB9501 luminometer (Berthold, Freiburg, Germany). The assays were performed in duplicate at least three times, and the mean and standard error were computed.

2.5. Vectors of ESCRT family proteins and DNA transfection

The cDNA of the endosomal sorting complex required for transport (ESCRT) family proteins was amplified from Huh7.5 cells by RT-PCR and cloned into pcDNA3.1-FLAG [13], an expression vector containing a CMV promoter and FLAG tag sequence in pcDNA3.1 (Invitrogen, Carlsbad, CA). For the expression of each ESCRT family protein, Huh7.5 cells were transfected with each ESCRT expression vector by using TransIT LT1 transfection reagents (Takara, Kyoto, Japan). The expression levels of the three ESCRT family proteins in

transfected Huh7.5 cells were monitored by immunoblotting using the anti-FLAG antibody (Sigma–Aldrich, St. Louis, MO).

2.6. Quantification of HCV core protein

HCV core protein in the cells or cell-culture supernatants was quantified by using a highly sensitive enzyme immunoassay (Ortho HCV antigen ELISA kit; Ortho Clinical Diagnostics). To determine the intra-cellular amounts of core, cell lysates were prepared as described by Schaller et al. [14].

2.7. Blocking of virus attachment and entry with anti-CD81 antibody

Blocking of virus attachment and entry with anti-CD81 antibody was performed essentially as described previously [9]. Huh7.5 cells (6×10^4 cells/well of a 24-well plate) were pre-treated with anti-CD81 antibody (clone JS-81; BD Biosciences) or an isotype-matched control antibody (purified mouse IgG1, isotype control; BD Biosciences) as indicated for 1 h. Cells were then infected with the reporter viruses for 6 h. The viruses were removed, and then the culture medium was replaced with complete DMEM. On day 2 post-infection, the cells were lysed with a passive lysis buffer as mentioned above. The efficiency of infection was monitored by measuring the luciferase activity of the cell lysate.

2.8. Transfection of microRNA inhibitor

Huh7.5 cells were electroporated with luciferase reporter HCV RNA as mentioned above, and then the cells were seeded in a well of a 24-well plate. To analyze the effect of inhibition of microRNA (miR), both a specific miRNA inhibitor (Anti-miR™ miRNA) and a non-targeting negative control (Anti-miR™miRNA Inhibitors—Negative Control) were purchased from Ambion, Inc. 50 pmol of a specific miRNA inhibitor or negative control were transfected into luciferase reporter RNA-electroporated Huh7.5 cells by using a siPORT™ NeoFX™ Transfection Agent (Ambion) according to the manufacturer's instructions. At 48 h post-transfection, the cells were harvested, and viral replication was determined by luciferase assay of the cell lysate.

2.9. Polyions

The polyanions heparin (mol. wt. 3000), dextran sulfate (mol. wt. 50,000) and polyvinyl sulfate (mol. wt. 150,000), and the polycations polybrene (mol. wt. 3000), DEAE-dextran (mol. wt. 100,000), and poly-L-lysine (mol. wt. 500,000) (all purchased from Sigma) were dissolved in PBS.

3. Results

3.1. Construction and characterization of luciferase reporter HCV

To construct a reporter HCV that can permit easy monitoring of both virus production and intra-cellular viral growth kinetics, we constructed the bicistronic HCV constructs by inserting a luciferase reporter gene into the 5′ end of the coding sequence of the JFH1 or J6/JFH1 full-genome plasmids clone as shown in Fig. 1A. In the transcript derived from bicistronic reporter HCV clone, the HCV and EMCV IRESs are responsible for the translation of the luciferase protein and all HCV proteins, respectively. A reporter construct with NS5B GDD to GND mutation, which disrupts viral polymerase function, was also constructed by site-directed mutagenesis, and served as a negative control for viral genome replication. To examine the replication level of reporter HCVs, we prepared the RNAs from each construct by *in vitro* transcription, and then transfected them into Huh7.5 cells by an electroporation technique. The viral replication was quantified up to 10 days post-transfection by using an HCV core-specific ELISA and luciferase reporter assay. As shown in Fig. 1B, the transfection of RNAs of both the JFH1/Luc and J6/JFH1/Luc reporter clones induced intra-cellular HCV core protein expression, which peaked on day 2 post-transfection. Both JFH1/Luc and J6/JFH1/Luc showed similar kinetics, and the high level core protein expression continued until day 10 post-transfection. As expected, the GND mutant exhibited 100-fold lower intra-cellular core protein expression on day 2 post-transfection. The level of core expression by the GND mutant continued to decline thereafter, and fell below the detection limit on day 10 post-transfection. As shown in Fig. 1C, both JFH1/Luc and J6/JFH1/Luc induced similar levels of luciferase activity in Huh7.5 cells at 4 h after electroporation. This result indicated that both RNAs were electroporated with similar efficiency because RNA replication had not started at that time and all the luciferase was translated from the input RNA. At 4 days post-electroporation, the luciferase activities of both JFH1/Luc and J6/JFH1/Luc were 10-fold greater than those measured at 4 h after electroporation. Subsequently, JFH1/Luc and J6/JFH1/Luc showed almost the same kinetics of luciferase activity until 10 days post-transfection. At 3 days post-electroporation, both JFH1/Luc and J6/JFH1/Luc electroporated cells were stained with HCV-positive patient sera, and the rate of intra-cellular replication was then visualized using immunofluorescent microscopy as previously reported [12]. As a result, the HCV-positive rates were 17% and 19% for JFH1/Luc and J6/JFH1/Luc, respectively (Fig. 1D). These results indicated that the luciferase activity of reporter HCV-transfected cells reflected the intra-cellular viral replication, and also suggested that both JFH1 and J6/JFH1 had similar intra-cellular replication ability in Huh7.5 cells.

3.2. Production of cell-free infectious progeny virions in luciferase reporter HCV RNA-transfected cells

Next, we assessed the potential of the reporter HCV to produce infectious progeny virions. Huh7.5 cells were electroporated with the reporter RNAs, and the culture supernatant was collected at various time points. To analyze the release of progeny virions from the reporter RNA-electroporated cells, the amounts of core protein in culture supernatants were

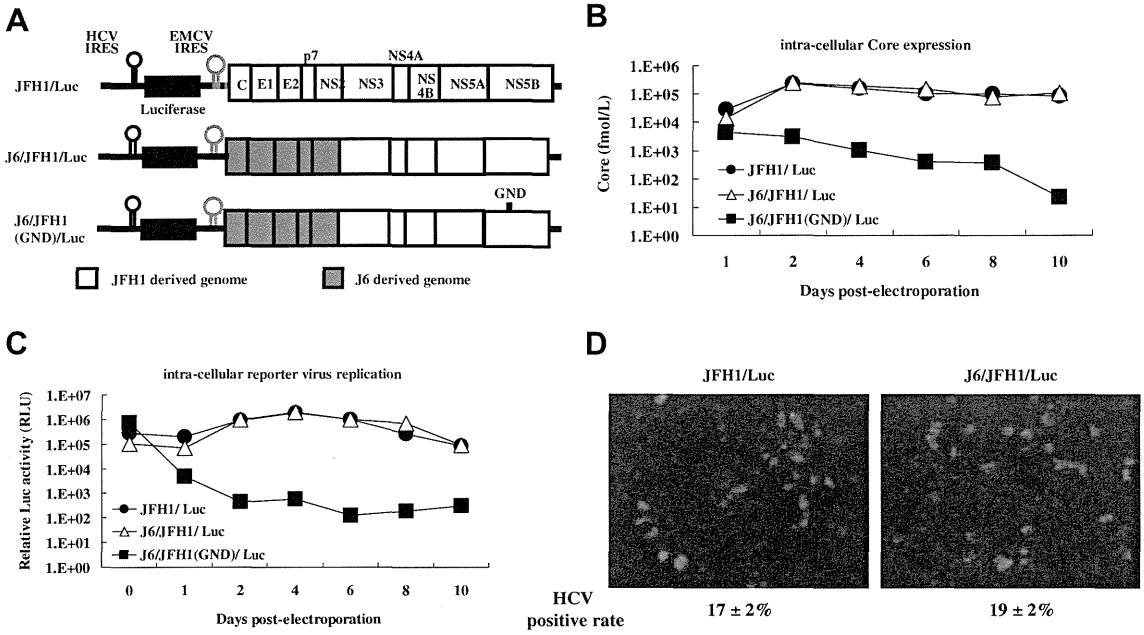

Fig. 1. Schematics of luciferase reporter HCV in this study. (A) Organization of luciferase reporter HCV. The luciferase gene is depicted as a black box. The JFH1-derived open reading frame and J6-derived open reading frame are depicted as a gray box and white box, respectively. As a negative control, a GND mutation was introduced to NS5B RdRp. (B, C) Virus replication kinetics in Huh7.5 cells of luciferase reporter HCV. The cells were electroporated with luciferase reporter RNA as described in Materials and methods, and the cells were assayed for core protein ELISA (B) and luciferase activity (C) at intervals as indicated. The assays were repeated at least three times, and the mean values are presented. Huh7.5 cells electroporated with JFH1/Luc or J6/JFH1/Luc RNA were subjected to indirect immunofluorescence analysis at 3 days post-electroporation (D). Cells were incubated with an HCV-infected patient's serum followed by FITC-labeled goat anti-human IgG (green). In parallel, the cells were stained with Hoechst 33342 to visualize the nuclei (blue). The HCV-positive rate was calculated by counting the number of HCV-positive cells among the total cells, and the data represent the means and SE of three independent experiments.

analyzed by ELISA. As shown in Fig. 2A, electroporation of both reporter viral RNAs with Huh7.5 cells released the HCV core protein into the culture supernatants. The levels of core protein released from both reporter HCV RNAs peaked at 6 days post-electroporation. The amount of core protein of the J6/JFH1/Luc supernatants was 2–4 fold greater than that of JFH1/Luc among all the time points tested. In parallel, to analyze the infectivity of progeny virions produced from reporter RNA-electroporated cells, these supernatants were used as inocula for naïve Huh7.5 cells. The cells inoculated with these supernatants were harvested at 48 h post-inoculation, and the luciferase activity of the cell lysate was analyzed (Fig. 2B). These supernatants infected naïve Huh7.5 cells, and transduced luciferase activity in the cells. The infectious virus of both reporter HCVs was initially detected on day 2 and peaked on day 4 post-electroporation. However, the infectivity was decreased after day 6 post-electroporation. Furthermore, the infectivity of J6/JFH1/Luc supernatants was significantly higher than that of JFH1/Luc (approximately 10-fold). To compare the luciferase activity and the virus titer, we

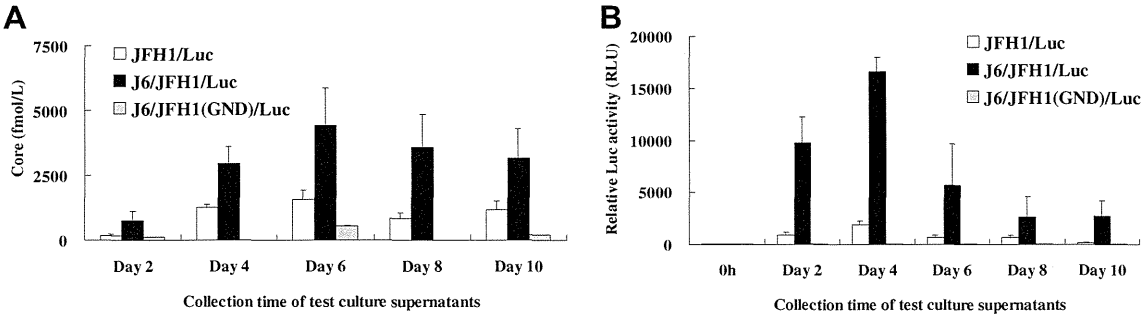

Fig. 2. Progeny virus production from luciferase reporter RNA-transfected Huh7.5 cells. The cells were electroporated with luciferase reporter RNA as described in Materials and methods, and culture supernatants of the cells were collected at the indicated time points. The amount of progeny virus in the supernatant was measured by the HCV core protein ELISA. (A) In parallel, the supernatants were added to naïve Huh7.5 cells. At 48 h post-addition, the cells were lysed, and assayed for luciferase activity to assess the infectivity of progeny virus from reporter HCV RNA. (B) The assays were repeated at least three times, and the mean values are presented.